

COMMITTEE CERTIFICATION OF APPROVED VERSION

The committee for Erik Justin Shank certifies that this is the approved version of the following dissertation:

Role of the Ventral Tegmental Area, Cannabinoid Receptors and GABA Neurons in Motor Activity

Committee:

Kathryn A. Cunningham, Ph.D., Chair

Joel P. Gallagher, Ph.D.

Kenneth M. Johnson, Ph.D.

Billy R. Martin, Ph.D.

Cheryl S. Watson, Ph.D.

Dean, Graduate School

**Role of the Ventral Tegmental Area, Cannabinoid Receptors
and GABA Neurons in Motor Activity**

by
Erik Justin Shank, B.S.

Dissertation
Presented to the Faculty of The University of Texas Graduate School of
Biomedical Sciences at Galveston
in Partial Fulfillment of the Requirements
for the Degree of

Doctor of Philosophy

Approved by the Supervisory Committee

Kathryn A. Cunningham, Ph.D.

Joel P. Gallagher, Ph.D.

Kenneth M. Johnson, Ph.D.

Billy R. Martin, Ph.D.

Cheryl S. Watson, Ph.D.

May, 2007
Galveston, Texas

Key words: Marijuana, Disinhibition, Mesoaccumbens

© 2007, Erik Justin Shank

Dedicated to those whose strong faith is based on the known and the ever-powerful unknown. May we never forget that the most important knowledge to be gained is that which cannot be currently explained.

ACKNOWLEDGEMENTS

I would like to first acknowledge my wife and my immediate family. They have given me the fortitude, faith and energy to endure these last few trying years. Without their faith and belief in me, I would have never had the courage to even entertain the idea of attempting this path. I would also like to thank my maternal grandparents (Anton und Anneliese Rebholz), my paternal grandparents (William and Marian Shank) as well as my newest grandparents (Robert and Shirley Gurganious) for their critical lessons of enduring the past, they have all been a tremendous inspiration to me and I hope I make a proud addition to their legacies. Lastly, I would like to thank my mentor Kathryn A. Cunningham for her tremendous ability and experience, which has benefited me in many different ways.

Role of the Ventral Tegmental Area, Cannabinoid Receptors and GABA Neurons in Motor Activity

Publication No. _____

Erik Justin Shank, Ph.D.

The University of Texas Graduate School of Biomedical Sciences at Galveston, 2007

Supervisor: Kathryn A. Cunningham

Illicit abuse of psychoactive substances, including marijuana, continues to be a serious problem in our society and therefore cultivating a more thorough understanding of the neuroanatomical and neurochemical substrates underlying drug abuse is needed. Characterizing specific brain nuclei that are integral components of brain reward circuits, such as the ventral tegmental area (VTA), may offer important insights into modulation of behaviors associated with drug abuse. The VTA includes DA-containing and GABA-containing neurons which provide important forebrain control over the limbic system. The present series of studies explored these VTA neurons from two perspectives: First, we explored the VTA as a potential site of action for cannabinoid receptors (CB₁R) and provide the first detailed analysis of the distribution of CB₁R throughout the various subnuclei and across the rostrocaudal extent of the VTA. We demonstrated that CB₁R populations have postsynaptic localization in the VTA, and a rostrocaudal gradient of expression in the interfascicular nucleus, which expressed the highest level of CB₁R in the VTA subnuclei. Second, we explored the prospect that specific ablation of a subset of VTA neurons, those GABA-containing neurons that possess μ -opioid receptors, play an important role in the generation of motor behavior. Ablation of GABA neurons following intra-VTA administration of the selective toxin dermorphin-saporin was associated with elevated spontaneous locomotor activity at day 7 that normalized to basal levels by day 14 after treatment. Despite this normalization motor hyperactivity induced by the well-characterized psychostimulant cocaine was significantly elevated in keeping with the

hypothesis that loss of GABAergic innervation in the VTA sensitizes to the neurochemical actions of cocaine. Collectively, our results demonstrate a new localization of CB₁R in the VTA and the behavioral impact of GABA-containing neuron ablation in the VTA. These data add to growing evidence of the impact of psychoactive substances on neuroanatomical substrates, such as the VTA.

TABLE OF CONTENTS

Acknowledgements	iv
Abstract	v
List of Figures	ix
List of Abbreviations	xi
Chapter 1. Introduction	
Drug Abuse	1
Marijuana	2
A Major Brain Circuit of Reward	2
Discovery of Cannabinoid Receptors in the Brain	3
Discovery of Endogenous Cannabinoid Agonists and the Development of Synthetic CB₁R Ligands	3
CB₁ Receptor	4
CB₂ Receptor	5
VTA as a Site of Action for Cannabinoid Agonists	6
GABA Neurons of the VTA	7
Overall Goals	7
Chapter 2. Localization of Cannabinoid CB₁ Receptors in Subnuclei of the Ventral Tegmental Area	
Abstract	8
Introduction	9
Materials and Methods	11
Results	14
Discussion	25
Chapter 3. Selective Ablation of Neurons Expressing μ-Opioid Receptors in the Ventral Tegmental Area: Increased Spontaneous Locomotor Activity and Cocaine Hyperactivity	
Abstract	29
Introduction	30
Materials and Methods	32
Results	38
Discussion	51

Chapter 4. Overall Conclusions

Introduction	55
Overall Summary	58

LIST OF FIGURES

	Page
Figure 1. CB ₁ R Gene Expression in Rat VTA Tissue	15
Figure 2. Blocking Peptide Eliminates CB ₁ R-IR	16
Figure 3. CB ₁ R-IR Expression Throughout the Rat Brain	18
Figure 4. Rostral VTA CB ₁ R-IR Expression	20
Figure 5. Middle VTA CB ₁ R-IR Expression	21
Figure 6. Caudal CB ₁ R-IR Expression	23
Figure 7. VTA CB ₁ R-IR Expression	24
Figure 8. Intra-VTA Dermorphin-Saporin (Day 7 pretreatment) Mean Increases Total Ambulation	38
Figure 9. Elevated Ambulation at Day 7 after Intra-VTA Dermorphin-Saporin	39
Figure 10. Intra-VTA Dermorphin-Saporin (Day 14 pretreatment) Increases Mean Total Ambulation	40
Figure 11. Elevated Ambulation at Day 14 after Intra-VTA Dermorphin-Saporin	41
Figure 12. Intra-VTA Dermorphin-Saporin Lesions GABA-containing Neurons	42
Figure 13. Intra-VTA Dermorphin-Saporin Appears to Decrease GAD-67-IR	44
Figure 14. Intra-VTA Dermorphin-Saporin Appears to Decrease μ -Opioid Receptor-IR	45
Figure 15. Intra-VTA Dermorphin-Saporin Appears to Have No Effect on Tyrosine Hydroxylase	46

Figure 16. Elevated Baseline Activity with DS-pretreatment Predicts Elevated Cocaine-induced Locomotor Activity	47
Figure 17. Elevated Baseline Activity with DS-pretreatment Predicts Elevated Cocaine-induced Locomotor Activity	48
Figure 18. Combination of Intra-VTA Dermorphin-Saporin (Day 14 pretreatment) and Cocaine Challenge Increase Mean Total Ambulation	49
Figure 19. Combination of Intra-VTA Dermorphin-Saporin (Day 14 pretreatment) and Cocaine Challenge Increase Mean Total Ambulation across 60 min	50

LIST OF ABBREVIATIONS

2-AG	2-arachidonyl glycerol
5-HT	Serotonin / 5-hydroxytryptamine
5-HT _{1A} R	Serotonin 1A receptor
5-HT _{2A} R	Serotonin 2A receptor
5-HT _{2C} R	Serotonin 2C receptor
Δ^9 -THC	Delta-9-tetrahydrocannabinol
ANOVA	Analysis of variance
ASN	Antisense
BDNF	Brain-derived Neurotrophic factor
BG	Basal ganglia
BP	Base pair
BS	Blank-saporin
DA	Dopamine
CB ₁ R	Cannabinoid receptor 1
CB ₂ R	Cannabinoid receptor 2
CPP	Conditioned place preference
C _t	Crossing threshold
DAB	3,3'-diaminobenzidine
DS	Dermorphin-saporin
FR	Fascicular retroflexus
GABA	Gamma-aminobutyric acid
GAD-67	Glutamic acid decarboxylase-67
GPCR	G-protein coupled receptor
IF	Interfascicular nucleus
IP	Intraperitoneal
IPN	Interpeduncular nucleus
IR	Immunoreactivity
MP	Mammillary peduncle

NAc	Nucleus accumbens
PIF	Parainterfascicular nucleus of the ventral tegmental area
PBP	Parabrachial pigmented nucleus of the ventral tegmental area
PBS	Phosphate buffered saline
PBS-T	Phosphate buffered saline containing 0.4% Triton-X
PFC	Prefrontal cortex
PN	Paranigral nucleus of the ventral tegmental area
ROI	Region of interest
Sal	Saline
SC	Subcutaneous
SD	Standard deviation
SN	Sense
SEM	Standard error of the mean
TH	Tyrosine hydroxylase
T _m	Melting temperature
VTA	Ventral tegmental area

CHAPTER 1

Introduction

Drug Abuse

Illicit drug abuse continues to be one of the most serious problems in American society, resulting in “more deaths, illnesses and disabilities than any other preventable health condition” (Robert Wood Johnson Foundation, 2001). The estimated economic burden associated with illegal drug use in the United States has grown drastically in the last few years, from \$107.6 billion in 1992 to \$181 billion in 2002, a result of primary health care expenses, lost job productivity, and costs associated with intervention and the rising costs of the criminal justice system (Office of Drug Control Policy, 2004). Alarming, illicit drug use is currently a greater economic burden to American society than obesity (\$99 billion per year), Alzheimer’s disease (\$100 billion per year), or cigarette smoking (\$138 billion per year, Office of Drug Control Policy, 2004). Even more important than the massive economic burden is the countless personal cost associated with the loss of quality of life for families and friends impacted by the devastation caused by drug addiction. Furthermore, constant debate rages among the American public, U.S. Government, and medical/scientific communities concerning the optimal care and/or feasible solutions to this evergrowing epidemic. One important aspect certainly is cultivating a better understanding of the mechanisms of action of abused drugs is critical to development of a greater number of pharmacotherapies with greater efficacy for drug abuse and addiction.

Marijuana

The psychoactive plant marijuana is undoubtedly the most abused illicit drug in the world (SAMHSA, 2003), a fact that emphasizes the pressing need to understand its mechanisms of action and to gain advantage to managing its psychological and physiological effects and marijuana dependence. In fact, roughly 6.2% (or 14.6 million) of Americans are estimated to have used marijuana at least once during the month previous to being surveyed during 2002 and a third of these reported heavy marijuana

use, characterized by use on approximately 20 or more days of use during the last month (SAMHSA, 2003). The acute effects of marijuana include euphoria, distorted perception, memory impairment and disrupted motor coordination (Ameri, 1999). One of the active alkaloids in marijuana, delta-9-tetrahydrocannabinol (Δ^9 -THC), is one of approximately 60 similar molecules found naturally in the *Cannabis sativa* plant (Ameri, 1999). These molecules are all members of the cannabinoid family of molecules, which are of interest in the treatment of pain, glaucoma, increasing appetite during chronic wasting, and also decreasing nausea associated with drug treatments (Kalant, 2001). In fact, the synthetic Δ^9 -THC (dronabinol) is in use in the United States for the treatment of nausea and vomiting associated with cancer chemotherapy and to increase appetite in AIDS patients (Mechoulam and Hanu, 2001). Clearly, understanding the manner through which cannabinoids operate within the CNS is important for the development of treatment modalities for marijuana abuse and dependence but also for gaining an understanding of the potential therapeutic utility of cannabinoid ligands as medications.

A Major Brain Circuit of Reward

One common feature of all drugs of abuse including cannabinoids is the modulation of neurotransmission within the mesoaccumbens dopamine (DA) pathway or 'reward pathway' which originates in DA cell bodies of the ventral tegmental area (VTA) and terminates in the nucleus accumbens (NAc). Increased DA release in the NAc is induced by psychoactive drugs from different drug classes (Di Chiara and Imperato, 1988b) via a multitude of distinct neural mechanisms. In fact, the natural cannabinoid agonist Δ^9 -THC and the synthetic cannabinoid agonist WIN55,212 have been reported to increase DA overflow in the NAc after systemic injection (Gardner and Vorel, 1998; Tanda et al., 1997; Tanda and Goldberg, 2003), which may be related to cannabinoid-evoked increases in firing rates and burst firing of VTA DA neurons (French, 1997). Additionally, significant increases in NAc DA levels are observed after acute administration of psychostimulants such as cocaine (Di Chiara and Imperato, 1988b). Therefore, the mesoaccumbens DA system is an important circuit in reward and is activated by drugs of abuse such as cannabinoids and psychostimulants.

Discovery of Cannabinoid Receptors in the Brain

A significant advancement in the cannabinoid field was the initial discovery of binding sites for Δ^9 -THC in rat brain tissue (Devane et al., 1988) and the description of cannabinoid receptor distribution in the brain (Herkenham et al., 1991b). These and other reports of critical molecular genetic studies (Matsuda et al., 1990; Munro et al., 1993) laid the foundation for the emergence of two major cannabinoid receptor subtypes (CB₁R and CB₂R). The CB₁R are primarily localized in the CNS but have been localized in very low abundance in some peripheral tissues, including small intestine, liver, vascular endothelium, and immune system cells (Kunos et al., 2002; Pertwee, 1997; Salio et al., 2002). The CB₂R, on the other hand, is primarily localized to immune cells in the periphery (Munro et al., 1993), but has recently been discovered in various brain tissues in low abundance (Onaivi et al., 2006).

Discovery of Endogenous Cannabinoid Agonists and Development of Synthetic CB₁R Ligands

Characterization of the cannabinoid receptors led to the discovery of the first known endogenous cannabinoid lipid agonists and synthetic CB₁R ligands. The first endogenous lipid cannabinoid agonist (endocannabinoid) to be characterized in mammals was named “anandamide,” derived from the sanskrit word for inner bliss and tranquility (Devane et al., 1988). Subsequently, numerous other endogenous molecules have been characterized with affinity for cannabinoid receptors in neuronal as well as peripheral tissues (Hanus et al., 2001; Mechoulam et al., 1995; Sugiura et al., 1995). Discovery and characterization of the two principle cannabinoid receptors also led to the synthesis of novel cannabinoid ligands. For example, two tri-terpenoid cannabinoid agonists (CP55,940 and WIN55,212-2) were initially developed following the structure analysis and synthesis of Δ^9 -THC (Mechoulam and Gaoni, 1965a) as well as the highly potent tricyclic benzopyran analog HU-210 (Pop, 1999). Today’s compliment of cannabinoid research tools continues to increase with the discovery and development of many new endogenous and synthetic molecules known to have affinity for cannabinoid receptors.

CB₁ Receptors

The CB₁R is a G-protein coupled receptor (GPCR) which negatively couples through G_{i/o} proteins to adenylate cyclase and positively couples to mitogen-activated protein kinase (Yamamoto and Takada, 2000). The CB₁R is also known to modulate ion channels, including potassium and N- and P/Q-type calcium channels (Ameri, 1999). One known splice variant of the CB₁R, the CB₁A has been currently characterized (Shire et al., 1995), and both the native receptor and the splice variant are generated from the native CB₁R mRNA and not from distinct exons (Shire et al., 1995). Endogenous cannabinoids such as anandamide and 2-arachidonyl glycerol can be generated as a response to postsynaptic depolarization in a cascade of biochemical steps that result in a release of endocannabinoids to act as retrograde signaling molecules; released endocannabinoids are proposed to bind to CB₁R located on the presynaptic neuron (Wilson and Nicoll, 2001). The signaling mechanisms for initiating cannabinoid generation and subsequent cannabinoid release have not been fully elucidated, although several signals appear to trigger endocannabinoid production; currently, both a Ca²⁺-modulated pathway and a metabotropic glutamate receptor modulated mechanism have been reported to control endogenous cannabinoid release (Wilson and Nicoll, 2002).

Although the presynaptic (terminal) localization and retrograde signaling mechanisms of action of endocannabinoids have been more thoroughly characterized, there is also a growing body of evidence suggests that CB₁R mediates the postsynaptic actions of cannabinoids (Endoh, 2006; Hohmann et al., 1999; Kelly and Chapman, 2001; Kirby et al., 2000; Lopez-Redondo et al., 1997; Pickel et al., 2004; Rodriguez et al., 2001; Salio et al., 2002; Schweitzer, 2000). In particular, two postsynaptic mechanisms of cannabinoids have been characterized to date. For example, stimulation of CB₁R by application of WIN55,212 has been noted to hyperpolarize neurons in the nucleus tractus solitarius via a K⁺-dependent mechanism (Endoh, 2006), and in the CA1 region of the hippocampus via a Ca²⁺-dependent mechanism (Kirby et al., 2000). The CB₁R has also been localized to the postsynaptically by electron microscopy and immunohistochemical studies which show CB₁R protein expression within plasma membranes in somatodendritic profiles and within the cytoplasm of caudate putamen neurons (Rodriguez et al., 2001), NAc medium-sized spiny neurons (Pickel et al., 2004) as well as neurons in dorsal horn of the spinal cord (Salio et al., 2002). Thus the CB₁R appears to be

functionally important at both pre- and postsynaptic locations, and the VTA localization of CB₁R has yet to be adequately investigated despite the importance of this brain nucleus in reward processes.

The CB₁R mRNA and protein have been localized to many different brain regions, including the cerebellum, hippocampus, and basal ganglia (caudate putamen, globus pallidus, substantia nigra), brain regions important in reward, learning and motor control (Herkenham et al., 1991b). In contrast to the consistent and repeated observations of high levels of CB₁R mRNA and protein in these regions, the localization of CB₁R mRNA to the mesoaccumbens circuit, including the VTA and NAc is more controversial (Schlicker and Kathmann, 2001). Studies of CB₁R mRNA or protein expression and receptor binding studies of CB₁R do not specifically describe the VTA as a site of expression (Moldrich and Wenger, 2000; Patel and Hillard, 2003; Pettit et al., 1998; Tsou et al., 1998). However, the CB₁R radioligand ³H-CP55,940 was shown to bind to tissue sections of the VTA at levels comparable to other known G-protein coupled receptors (GPCRs; Herkenham et al., 1991b). Immunohistochemical localization of CB₁R in DA neurons of the VTA was described (Wenger et al., 2003) however the anatomical localization within the VTA was not described. A comprehensive demonstration of CB₁R protein expression throughout the VTA and its component subnuclei has not yet been described, therefore a primary goal of these studies is to use immunohistochemical techniques to describe the localization of CB₁R throughout the VTA.

CB₂ Receptors

The CB₂R is also a GPCR that is negatively coupled through G_{i/o} proteins to adenylate cyclase and positively coupled to mitogen-activated protein kinase (Ameri, 1999). The CB₂R only shares 44% sequence homology throughout the total protein and only 68% sequence homology within the transmembrane domains of the CB₁R (Munro et al., 1993). Furthermore, the localization of the CB₂R is markedly different from the CB₁R, which is primarily located in immune cells with particularly high levels found in the spleen (Munro et al., 1993; Schatz et al., 1997) and only small amounts detectable in the CNS (Onaivi et al., 2006). The signal transduction mechanisms are also distinct from the CB₁R in that ionotropic actions of CB₂R have not been reported (Felder et al., 1992).

VTA as a Site of Action for Cannabinoid Agonists

The VTA has been implicated as a prominent site of action of cannabinoid agonists. For example, systemic administration of Δ^9 -THC or the synthetic cannabinoid agonist WIN55,212-2 increased firing of VTA DA neurons and this effect was blocked by pretreatment with the cannabinoid antagonist SR141716a (French, 1997; French et al., 1997). The increases in VTA DA firing caused by cannabinoid agonists binding to CB₁R in the VTA may be due to inhibition of gamma-aminobutyric (GABA) neurotransmission allowing a disinhibition of DA neurons (Szabo et al., 2002). However cannabinoid agonists have also been found to inhibit glutamate neurotransmission in the VTA (Melis et al., 2004), thus suggesting potentially competitive mechanisms of action between inhibitory and excitatory inputs to VTA neurons. The potentially heterogeneous VTA CB₁R populations in the VTA that may differentially modulate neurotransmission and therefore these reports CB₁R populations warrant further study.

The VTA is not only heterogeneous in terms of resident neuronal populations and connectivity (Geisler and Zahm, 2005; Swanson, 1982c) but also may be in terms of behavioral function. This functional heterogeneity is becoming evident in terms cannabinoid-evoked behavior and protein expression after cannabinoid administration across rostral (anterior) and caudal (posterior) regions (Butovsky et al., 2005; Zangen et al., 2006). For example, administration of Δ^9 -THC into the caudal, but not rostral, VTA induced hyperactivity and supported both a conditioned place preference and self-administration (Zangen et al., 2006). Additionally, recent reports indicate that systemically-administered cannabinoids can differentially alter the expression levels of several cellular markers across VTA subnuclei. For example, chronic Δ^9 -THC (1.5 mg/kg, IP, per day for 7 days) administration preferentially induced brain-derived neurotrophic factor (BDNF) expression in the caudal VTA (4-fold change) compared to the rostral VTA (1.7-fold change) (Butovsky et al., 2005). Thus, taken together, these data suggest that regional differences in the expression and actions of CB₁R in the VTA contribute to differential behavioral and molecular consequences of cannabinoid exposure.

Gamma-aminobutyric acid (GABA) Neurons of the VTA

Key regulatory components of the VTA are the inhibitory GABA inputs from local VTA GABA-containing interneurons and from GABA-containing projection neurons (Mathon et al., 2003; White, 1996). These neurons release the neurotransmitter GABA which binds to pre- (GABA_B) and postsynaptic GABA (GABA_A and GABA_B) receptors located on DA neurons to then inhibit the firing of DA neurons (Korotkova et al., 2004). The GABA-containing neurons in the VTA are also thought to express CB₁R protein (Schlicker and Kathmann, 2001) and therefore may mediate in part the behavioral effects of cannabinoid agonist administration. Understanding the inhibitory control of GABA-containing neurons in the VTA is critical in understanding both basic reward pathway function as well as behavior elicited by drugs of abuse.

Overall Goals

The loci and mechanisms of cannabinoid actions in the VTA are unclear. One primary goal of this project is to develop a better understanding of the localization of CB₁R in VTA and the functional significance of these receptors in the VTA. We first utilized one of the first commercially available anti-CB₁R antibodies (CB1, N-15; sc-10066, Santa Cruz Biotechnology, Inc., Santa Cruz, CA) to characterize the localization of CB₁R protein within the VTA. Furthermore, based on evidence that CB₁R may modulate behavior via direct action on GABA-containing neurons, we examined the effects of selective ablation of GABA-containing neurons in the VTA on basal locomotor activity, mRNA and protein expression of μ -opioid receptors, glutamic-acid decarboxylase-67 (GAD-67). Additionally we examined the effects of loss of VTA GABA-containing neurons on hyperactivity induced by the psychostimulant cocaine. Developing a better understanding of VTA cannabinoid receptor localization and the modulatory contribution of GABA-containing neurons in basal and drug-evoked behaviors is critical to the development of a more thorough understanding of the mesocorticolimbic reward pathway.

CHAPTER 2

Localization of Cannabinoid CB₁ Receptors in Subnuclei of the Ventral Tegmental Area

ABSTRACT

A functional role for the cannabinoid CB₁R in the VTA has been described based upon behavioral and electrophysiological analyses, yet knowledge regarding CB₁R protein expression in the VTA is limited. The goal of the present study was to further confirm and detail the distribution of CB₁R protein throughout the rostrocaudal extent of the VTA using immunohistochemical detection. To this end, we utilized immunohistochemical techniques to explore the regional, subregional, and cellular distribution of CB₁R immunoreactivity (IR) throughout the VTA of male Sprague-Dawley rats. The CB₁R-IR was distributed in cellular-and fiber-like structures in component subnuclei (interfascicular nucleus, parabrachial pigmented nucleus, paranigral nucleus, parainterfascicular nucleus) of the VTA. Low-to-moderate numbers of CB₁R-IR positive cells were observed in subnuclei represented at rostral and middle levels, while moderate-to-high numbers of CB₁R-IR positive cells were found in the caudal VTA. The caudal interfascicular nucleus contained a rostrocaudal gradient of CB₁R-IR and the highest density of CB₁R-IR cells within the entire VTA. These data support observations that the VTA is anatomically heterogenous and suggest that the caudal interfascicular nucleus may be an especially important site of action for the generation of behaviors evoked by administration of the cannabinoids, such as Δ^9 -tetrahydrocannabinol in marijuana, the most abused illicit drug in the world today.

INTRODUCTION

The abuse liability and euphoric effects of marijuana in humans have been linked to a key psychoactive alkaloid Δ^9 -tetrahydrocannabinol (Δ^9 -THC) (Mechoulam and Gaoni, 1965b). Animal studies have characterized a myriad of motor, rewarding and aversive behavioral effects of Δ^9 -THC which have been recently shown to overlap with those of synthetic cannabinoid agonists such as WIN 55,212-2 and CP55,940 (Gardner, 2002). The mechanisms of action underlying the rewarding and reinforcing effects of cannabinoid agonists may include modulation of mesoaccumbens DA circuits as indicated by the observation that systemic administration of Δ^9 -THC or potent synthetic cannabinoid receptor agonists enhances DA release in axonal terminal regions of VTA neurons, including the nucleus accumbens (NAc; Cheer et al., 2004) and prefrontal cortex (PFC; Chen et al., 1990), in a calcium-, impulse- (French et al., 1997) and CB₁R-dependent manner (French, 1997; Gardner, 2002; Gardner, 2005). Actions within the VTA could account for cannabinoid-evoked DA efflux in forebrain regions given that CB₁R activation after systemic administration of cannabinoid agonists results in increased firing rates and burst firing of DA VTA neurons (French et al., 1997). In support of the possibility of the VTA as a site of action for cannabinoid agonists, microinjection of Δ^9 -THC into the posterior VTA evokes hyperactivity and a conditioned place preference (CPP; Zangen et al., 2006). Thus, direct or indirect actions of cannabinoids at CB₁R in the VTA could result in increased cell firing of DA VTA neurons and the subsequent increased DA release in forebrain and evocation of behavioral outcomes.

Despite the attractiveness of this hypothesis, a significant disparity exists. Although electrophysiological effects of cannabinoid agonists are observed upon application to the VTA (French et al., 1997; Gessa et al., 1998; Melis et al., 2004; Szabo et al., 2002), evidence of expression of a population of CB₁R mRNA or protein in neurons of the VTA is limited. Neither *in situ* hybridization studies of CB₁R mRNA expression or immunohistochemical and receptor binding studies of CB₁R protein expression mention the VTA as a site of expression (Moldrich and Wenger, 2000; Patel and Hillard, 2003; Pettit et al., 1998; Tsou et al., 1998). However, images published in studies of radiolabeled cannabinoid agonist (³H-CP55,940) binding in rat brain tissue clearly demonstrated and quantified the binding in the VTA (Herkenham et al., 1991a;

Herkenham et al., 1991b) at expression levels (1.46 pmol/mg protein) comparable to those of some common ionotropic receptors and even greater levels than most G-protein coupled receptors (Bowery et al., 1987; Greenamyre et al., 1984). Furthermore, the first documentation of CB₁R-immunoreactive (CB₁R-IR) protein detection in DA neurons of the VTA with antibody labeling was recently noted (Wenger et al., 2003). Wenger described experiments that indicate the expression of CB₁R in the VTA, however, the detailed anatomical localization of VTA CB₁R-IR has not been characterized and a thorough analysis of the distribution of CB₁R-IR in the VTA is necessary to fully understand the role of endogenous CB₁R in this important region of the reward circuit.

The VTA is located in the ventral portion of the mesencephalon and is comprised of the A10 DA population of mesencephalic catecholamine neurons (Dahlstrom and Fuxe, 1964). The VTA extends from the level of the supramammillary bodies caudally to linear raphe nucleus at the level of the pontine nucleus (German and Manaye, 1993a; Swanson, 1982b) and is divided based upon cytoarchitecture into multiple subnuclei (see **Figures 4-6**): the paranigral nucleus (PN), the parabrachial pigmented nucleus (PBP), the interfascicular nucleus (IF), and the parainterfascicular nucleus (PIF). The projection of VTA DA neurons to forebrain sites, such as the NAc, has been shown to differ among the subnuclei (Swanson, 1982a; Phillipson, 1979). For example, DA neurons in the PN, PBP, and IF comprise the largest population of VTA neuronal efferents to innervate the NAc and prefrontal cortex (PFC) (Swanson, 1982d). Thus, the VTA contains numerous levels of complexity, and a greater understanding of the differences across the individual subnuclei will allow important advances in understanding VTA neurotransmission. A critical advancement in delineating VTA neurotransmission is determining the differential distribution of receptors such as the CB₁R within the subnuclei of the VTA.

In the present study, confirmed the presence of CB₁R mRNA in tissue homogenates isolated from the VTA. We also validate the presence of CB₁R-IR in various brain areas known to express CB₁R and a specific distribution of the CB₁R within cells in subnuclei of the VTA (IF, interfascicular nucleus; PBP, parabrachial pigmented nucleus; PN, paranigral nucleus; PIF, parainterfascicular nucleus) using a CB₁R antibody (N-15, sc-10066, lot# F1903, goat polyclonal CB₁; Santa Cruz Biotechnology, Santa Cruz, CA) to characterize expression of the CB₁R in the VTA.

MATERIALS AND METHODS

Tissue Preparation

Naïve male Sprague-Dawley rats (n=3, Harlan Sprague-Dawley, Inc., Indianapolis, IN) weighing 275-300g were used. Rats were deeply anesthetized with pentobarbital (100 mg/kg, IP, Sigma) and perfused transcardially with phosphate buffered saline (PBS) followed by 3% buffered paraformaldehyde in PBS (500 ml/rat). After brain removal and post-fixation (2 hr) at room temperature, the brains were transferred to a 30% sucrose solution (4°C, 2 days) for cryoprotection, then rapidly frozen with crushed dry ice and stored at -80°C until sectioning. Free floating sections were processed as described below. All experiments were conducted in accordance with the National Institutes of Health *Guide for the Care and Use of Laboratory Animals* and with approval from the Institutional Animal Care and Use Committee.

Total RNA Extraction and Reverse Transcription

Naïve rats (n=3) were anesthetized using chloral hydrate (800 mg/kg, IP) and decapitated. The VTA tissue was microdissected using a method modified from Heffner and validated in our lab (Bubar et al., 2004; Heffner et al., 1980; Herin et al., 2005) and stored in RNAlater® (Ambion, Austin, TX) at -80°C. Total RNA from tissue was prepared using standard methods (RNAqueous®, Ambion). The quality of total RNA was verified by electrophoresis and spectrophotometry. Reverse transcription was performed using the TagMan® Reverse Transcription Kit (Applied Biosystems, Foster City, CA) and the Perkin Elmer GeneAmp® System 9600 (PE Biosystems, Foster City, CA). The reverse transcription program consisted of 25°C for 10 min, 48°C for 30 min, and 95°C for 5 min. Random hexamers were used to prime all reverse transcription reactions.

PCR

A 114bp (base pair) specific rat CB₁R encoding region was amplified by PCR using the sense primer 5'-GCTGCTGCTGTTTCATTGTGT-3' and the antisense primer 5'-CGTCTTCTGACGTGTGGATG-3'. Primers were designed using Primer 3 (http://frodo.wi.mit.edu/cgi-bin/primer3/primer3_www.cgi; Whitehead Institute for Biomedical Research; Rozen and Skaletsky, 2000). The amplification reaction was

carried out in a Perkin Elmer GeneAmp® System 9600 for 35 cycles. Each cycle consisted of denaturation for 15 sec at 94°C, annealing for 30 sec at 62°C, and an extension for 30 sec at 72°C. A final extension step at 72°C for 10 min terminated the amplification. PCR product was analyzed by electrophoresis using a 3% agarose gel.

Immunohistochemistry

Sections were processed in parallel throughout all immunohistochemical assays. Briefly, coronal sections (35 µm) containing the hippocampus [-4.5mm from Bregma] or VTA [rostral -5.0 mm, middle -5.5 mm, and caudal -6.0 mm from Bregma (Nocjar et al., 2002)] were taken from brains using a cryostat (Leica CM1850, Bannockburn, IL) kept at -20°C according to the atlas of Paxinos and Watson (2005). Standard procedures were employed for immunodetection (Frankel and Cunningham, 2002; McInvale et al., 2002). Briefly, following extensive washes, non-specific binding was blocked by incubating the tissue sections in 0.4% Triton X-100 in PBS containing 1.5% normal rabbit serum (Vector Laboratories, Burlingame, CA) for 1 hr, then in primary antibody (2 days, 4°C). The primary antibody was a polyclonal anti-CB₁R made in goat, used at a 1:500 dilution (N-15, Cat# sc-10066, lot# F1903; Santa Cruz Biotechnology, Santa Cruz, CA, which has been employed in numerous studies (Ashton et al., 2004a; Ashton et al., 2004d; Ashton et al., 2004b; Ashton et al., 2006a; Jiang et al., 2005; Smith et al., 2006). Following extensive PBS washing, sections were incubated in a secondary antibody solution (biotinylated goat anti-rabbit IgG, 1:400; Vector) for 1 hr, then in an avidin/biotin-horseradish peroxidase complex (ABC; Vectastain® Elite kit; Vector) for 1 hr. The sections were rinsed 3x in a Tris buffer (pH 7.6) followed by incubation in diaminobenzidine (0.5 mg/ml) with 0.005% H₂O₂. The chromagen reaction was terminated by placing the sections in PBS. Sections were mounted out of a 0.1% Drefits® solution onto slides previously coated with gelatin chrom alum. DPX (Fisher Scientific, Houston, TX) was used to coverslip the slides.

Antibody Validation

Several controls were employed to validate the specificity of the CB₁R antibody under the present immunohistochemical conditions. Staining in free-floating sections was assessed following either incubation of the primary antibody (1:500) or secondary

antibody alone (1:400). In addition, CB₁R immunoreactivity was assessed in tissue sections containing the hippocampus in which this particular CB₁R antibody (N-15, Cat# sc-10066, lot# F1903) and other CB₁R antibodies (Pettit et al., 1998; Tsou et al., 1998) have been well-characterized to stain a definitive pattern of cells in the molecular and polymorph layers of the dentate gyrus. In an additional control, we analyzed staining following preabsorbtion/co-incubation of the peptide (sc-10066-P, lot# D0805, Santa Cruz Biotechnology, Santa Cruz, CA) with the primary antibody (1:500). The preabsorbtion/co-incubation reaction was carried out in 300 µl of filtered PBS (primary antibody, 1:500; peptide 1:100) for 2 hr prior to the addition of the reagents to free floating sections and immunohistochemistry as described above. The specificity of this antibody has been previously determined in Western blot analyses; the antibody labeled a single band at 60 kDa (Jiang et al., 2005) and three bands at 53, 59 and 63 kDa (Ashton et al., 2004d) that correspond to the CB₁R and expression of all bands was completely blocked by preabsorption with the corresponding peptide antigen.

Quantification of VTA CB₁R Immunostaining

Digital images (3 images of 3 sections per area per animal, n=3) of CB₁R immunostaining were captured from coronal brain sections containing the VTA using an Olympus BX51 equipped with a Professional Hamamatsu digital camera (C4742-95; Hamamatsu, Bridgewater, NJ) interfaced to a personal computer and analyzed with the aid of SimplePCI software (version 6.0, Compix, Imaging Systems, Cranberry Township, PA). Identification of each rostral (-5.0 mm), middle (-5.5 mm), and caudal (-6.0 mm) VTA section as well as the VTA component subnuclei were determined and isolated in individual regions of interest (ROIs) by utilizing the location of the fasciculus retroflexus (fr) and mammillary peduncle (mp) as landmark structures (**Figures 4-6**) (Paxinos and Watson, 2005). Quantification was carried out bilaterally by automatically measuring the number of positive cells in photomicrographs of each ROI of each subnucleus of the VTA at each brain “level” (rostral, middle, caudal) by using SimplePCI 6.0. Low magnification (4x objective lens) images (**Figures 4-6**) were subdivided anatomically by Adobe Photoshop using the polygonal “lasso” tool into VTA subnuclei ROIs based upon the appropriate atlas images (**Figures 4-6**; Paxinos and Watson, 2005).

Each VTA ROI image area was automatically converted from pixels to square micrometers by using a calibration slide with the aid of the Simple PCI program. The number of positive cells was estimated by using a double-threshold technique based on average cell size and gray-scale intensity level (Wang and Johnson, 2005). Nonspecific staining as well as non-cellular staining was eliminated from quantification by only counting objects within a specific size range (~5 μ m to ~20 μ m diameter). An average value was calculated for each brain region (3 sections per area per animal, N=3); these values were then used to represent a “mean of means” of the regional value for all animals. Adobe photoshop was used to perform minor adjustments of color and detail contrast (Geisler and Zahm, 2005) and these adjustments were carefully performed consistently across all images. The extent of staining was expressed as a mean total count of labeled cells in the entire ROI within the VTA (see Results) and a mean total count of labeled cells normalized as cells/0.1mm² (**Figure 7**).

Statistical Analysis

The number of CB₁R-IR positive cells obtained across three sections for each VTA level (rostral, middle, caudal) and subnucleus (IF, interfascicular nucleus; PBP, parabrachial pigmented nucleus; PIF, parainterfascicular nucleus; PN, paranigral nucleus) per animal were averaged for each rat and then averaged again across all rats (n=3) to calculate a “mean-of-means.” A mixed model was fit (MIXED procedure in SAS, Version 8.2, SAS Institute, Cary, NC) to examine differences in the numbers of immunoreactive-positive (IR-positive) cells at two levels. One level compared relative number of cells within each subnucleus and the other level compared the relative number of cells throughout the three rostrocaudal levels (Bregma -5 mm, -5.5 mm, and -6.0 mm). We used the Tukey-Kramer procedure in MIXED to make pairwise comparisons (Singer, 1998).

RESULTS

CB₁R Transcripts

The RNA extracted from microdissections of the VTA was reverse-transcribed into cDNA and amplified using CB₁R specific primers. We identified a target band of the predicted size (114 bp, lane 2) based upon our primer specificity (**Figure 1**). We failed to

generate similar bands in PCR mixtures that contained all required reagents with the exception of the tissue sample (lane 3). The presence of the appropriate sized band indicates the presence of CB₁R transcripts in VTA tissue microdissected from rat brain tissue.

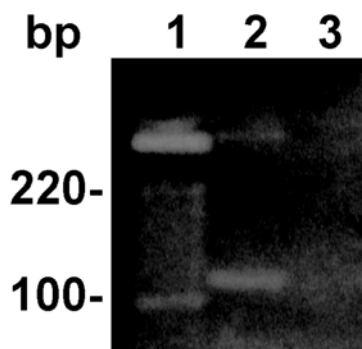


Figure 1. CB₁R Gene Expression in Rat VTA Tissue

PCR indicates the presence of CB₁R RNA in tissue isolated from the VTA. Lane 1: molecular weight standards; Lane 2: CB₁R receptor specific band (114 bp); Lane 3: PCR reaction without sample RNA added.

CB₁R Antibody Validation

Cells labeled by the CB₁R antibody were detected in areas of the brain previously reported, for example, the hippocampus (**Figures 2A-B**, Moldrich and Wenger, 2000; Pettit et al., 1998; Tsou et al., 1998). **Figures 2A** (arrowheads) and **2B** show immunopositive cells in the dentate area of the hippocampus, with most of the labeled cells located between the granule and polymorph layers. **Figures 2D** and **2E** show immunopositive cells in the ventral tegmental area. The CB₁R immunoreactivity was not observed in the hippocampus (**Figure 2C**, arrowheads) or the VTA (**Figure 2F**) after analyses conducted with the CB₁R antibody preincubated with a 5x excess of the CB₁R peptide. Control experiments indicate a complete absence of specific labeling of cells by either the primary antibody (**Figure 2G**) or secondary antibody alone (**Figure 2H**) in the VTA suggesting that the observed immunoreactivity (IR) was specific to the combination of CB₁R specific primary and secondary antibodies.

Figure 2.

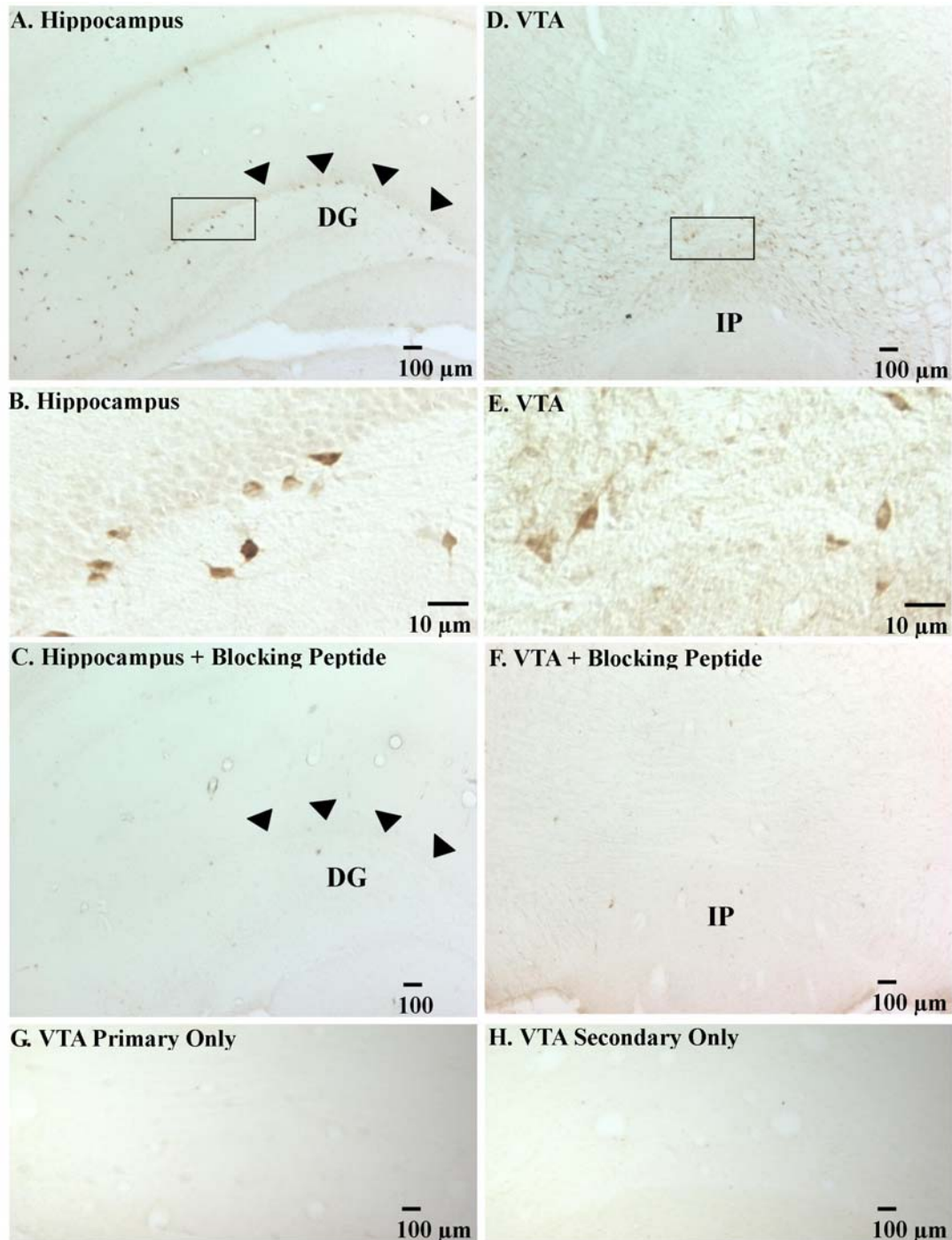


Figure 2. Blocking Peptide Eliminates CB₁R-IR

Representative brightfield photomicrograph of CB₁R-IR (brown staining) in coronal sections of the VTA and hippocampus (100x magnification). **A.** Arrowheads indicate the landmark division between the molecular and polymorph layers of the dentate gyrus of the hippocampus (-4.8 mm relative to bregma). **B.** High magnification (400x) image displays CB₁R-IR (brown staining) in the boxed region of the hippocampus section in

2A. C. Representative brightfield photomicrograph indicates an absence of staining in the hippocampus when the antibody was preabsorbed/incubated with the blocking peptide (See Methods) with arrowheads indicating the landmarks identified in **2A. D.** Representative brightfield photomicrograph indicates the expression of CB₁R-IR in a coronal section of the caudal VTA (-6.0 mm relative to Bregma; 100x magnification). **E.** High magnification (400x) image displays CB₁R-IR in the boxed region of the caudal VTA section in **2D. F.** Representative brightfield photomicrograph indicates an absence of staining in the caudal VTA subnuclei when the antibody was preabsorbed/incubated with the blocking peptide (See Methods). **G.** Representative brightfield photomicrograph indicates an absence of staining in the VTA when the tissue sections were incubated with primary anti-CB₁R antibody only (Santa Cruz Biotechnology, Santa Cruz, CA; sc-10066; lot# F1903). **H.** Representative brightfield photomicrograph indicates an absence of staining in the VTA when the tissue sections were incubated with secondary antibody only (goat anti-rabbit IgG, 1:400; Vector) IP = interpeduncular nucleus, DG = dentate gyrus.

CB₁R Immunoreactivity throughout the rat brain

Cells of different size and morphology clearly expressed CB₁R-IR throughout various brain nuclei analyzed that have been previously identified to express CB₁R (Herkenham et al., 1991b), including the motor cortex (**Figure 3A**), NAc shell (**Figure 3B**), dorsal raphe nucleus (**Figure 3C**) and the medial septal nucleus (**Figure 3D**). Immunopositive labeling was detected in cellular-and fiber-like structures (**Figure 3**) and cells of different size and shape were labeled (**Figure 3A**, open versus closed arrow). Labeling was also detected along processes in several areas (For example, **Figure 3A-C**).

CB₁R Immunoreactivity in the VTA

Cells of different size and morphology clearly expressed CB₁R-IR throughout all subnuclei within the rostral (**Figure 4**), middle (**Figure 5**), and caudal VTA (**Figure 6**). Immunopositive labeling was detected primarily in cell bodies (**Figures 4-6**), but CB₁R-IR was also detected in processes as well (**Figures 4F and 5D**), although less frequently. Additionally, small clusters of CB₁R-IR were detected along processes (**Figure 6F**). Clustering along processes was most commonly detected in the rostral level of the VTA within lateral subnuclei, such as the PBP (**Figure 4D-F**).

Figure 3.

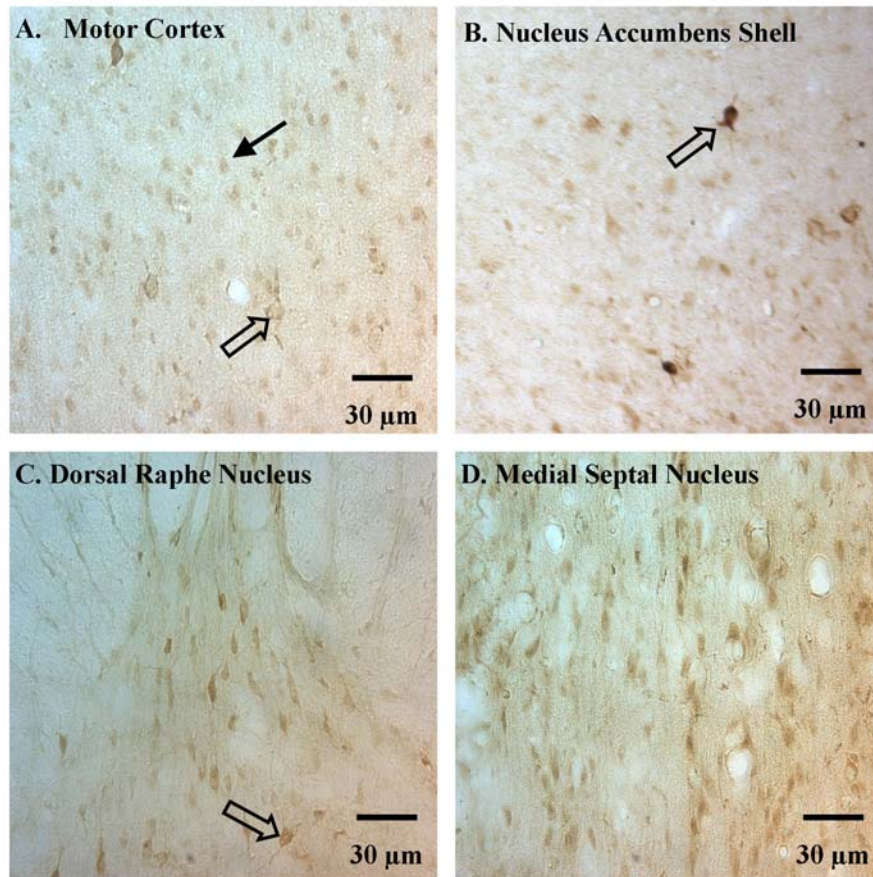


Figure 3. CB₁R-IR Expression Throughout the Rat Brain

Representative brightfield photomicrograph of CB₁R-IR (brown staining) in coronal sections of brain areas previously shown to have CB₁R-IR protein expression. **A.** High magnification (200x) image displaying CB₁R-IR (brown staining) in the motor cortex (-1.8 mm Bregma). Closed arrow indicates smaller-sized cell, the open arrow indicates larger cell with staining throughout cell and along processes. **B.** High magnification (200x) image displaying CB₁R-IR in the NAc shell (2.0 mm Bregma). The open arrow indicates staining on both cell body as well as processes. **C.** High magnification (200x) image displaying CB₁R-IR in the dorsal raphe nucleus (-7.32 mm Bregma). The open arrow indicates staining on cell body as well as processes. **D.** High magnification (200x) image displaying CB₁R-IR in the medial septal nucleus (2.0 mm Bregma).

CB₁R Immunoreactivity in the Rostral VTA

Profiles of CB₁R-IR indicated a rostrocaudal gradient with low-to-moderate numbers of CB₁R-IR positive cells in the ROIs in the rostral VTA. Relatively few CB₁R-IR positive cells were detected in two subnuclei (interfascicular nucleus, IF; parabrachial

pigmented nucleus, PBP) found in the rostral VTA (**Figures 4A-F**). Total labeled cells were low [n=3 brains, n=3 sections per brain area; total 14 ± 3 (SEM) labeled neurons] within the ROI in the IF as well as moderate within the ROI in the PBP [n=3 brains, n=3 sections per brain area; total 73 ± 23 (SEM) labeled neurons]. Analyses of the parainterfascicular nucleus (PIF) and paranigral nucleus (PN) were not included as these subnuclei were not present at this plane at these coordinates.

CB₁R Immunoreactivity in the Middle VTA

Moderate-to-high levels of CB₁R-IR positive cells were detected within analyzed sections of the middle VTA (**Figures 5A-F**). CB₁R-IR positive cells were present in high quantities [n=3 brains, n=3 sections per brain area; total 93 ± 7 (SEM) labeled cells] in the ROI of the PIF and moderate quantities in the PBP [n=3 brains, n=3 sections per brain area; total 56 ± 18 (SEM) labeled cells], IF [n=3 brains, n=3 sections per brain area; total 28 ± 5 (SEM) labeled cells] and PN [n=3 brains, n=3 sections per brain area; total 34 ± 4 (SEM) labeled cells]. The overall staining of the middle PBP of the VTA looked very similar to that observed in the rostral VTA, but a higher number of cells were detected (**Figure 7**).

CB₁R Immunoreactivity in the Caudal VTA

The caudal VTA contained the highest number of CB₁R-IR cells compared to rostral and middle VTA levels within all sections for all three brains analyzed (**Figures 4-6**). CB₁R-IR positive cells were detected in high numbers throughout the ROIs in the caudal PN [n=3 brains, n=3 sections per brain area; total 95 ± 11 (SEM) labeled cells], PBP [n=3 brains, n=3 sections per brain area; total 138 ± 4 (SEM) labeled cells], and PIF [n=3 brains, n=3 sections per brain area; total 96 ± 8 (SEM) labeled cells], and in moderate numbers in the IF [n=3 brains, n=3 sections per brain area; total 49 ± 4 (SEM) labeled cells]. There was also a clear morphological difference between the CB₁R-IR observed cells in the caudal IF and the other CB₁R-IR positive cells throughout the VTA. CB₁R-IR in the caudal IF was observed primarily on cell somata (**Figures 6A-F**) while both somata and processes were stained in other subnuclei. The CB₁R-IR positive cells observable within the IF also appeared to be more uniform in size and appeared to exhibit

more spherical shapes overall as compared to the more stellate cells observed in the PBP (Figures 6A-F).

Figure 4.

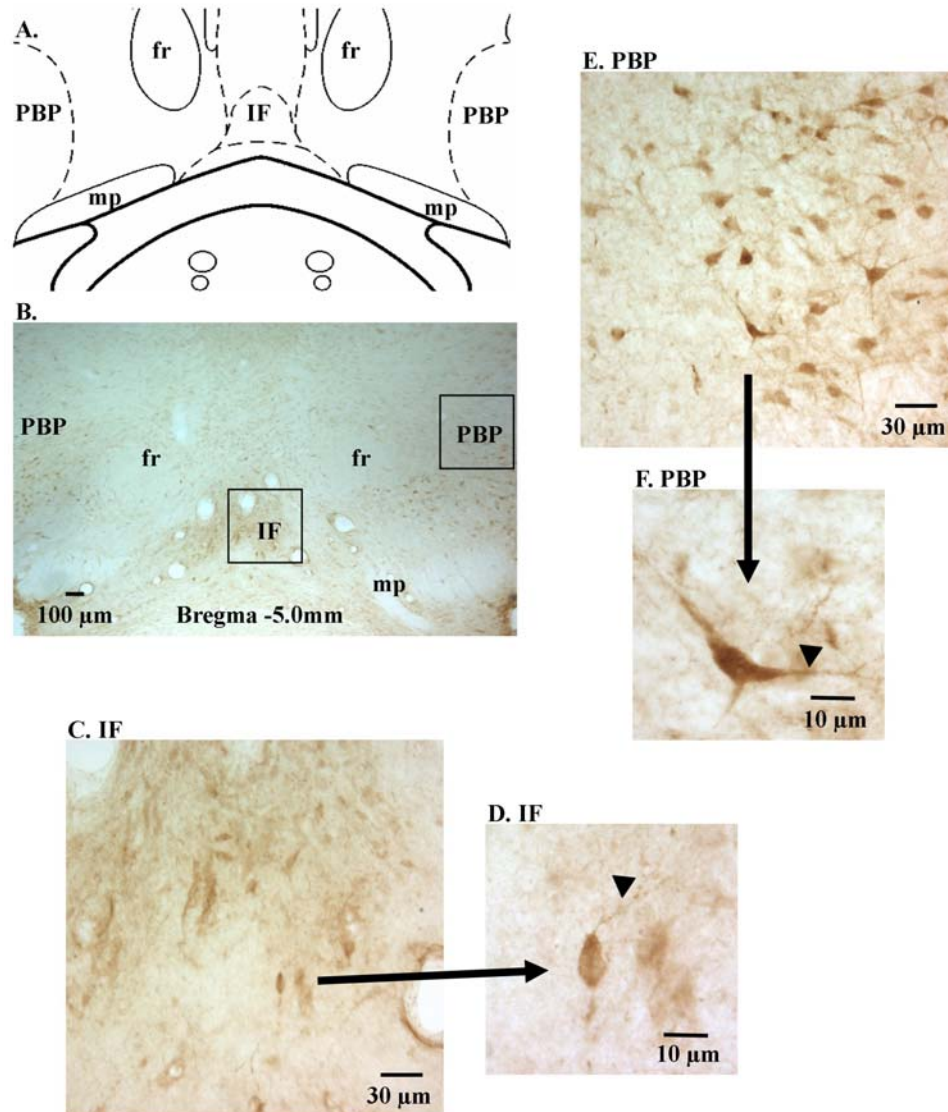


Figure 4. Rostral VTA CB₁R-IR Expression

Schematic representation of the rostral VTA at -5.0 mm Bregma (adapted from Paxinos and Watson, 2005). Landmark structures and subnuclei included: fasciculus retroflexus (fr), interfascicular nucleus (IF), parabrachial pigmented nucleus (PBP), and mammillary peduncle (mp). **A.** Representative atlas image of the rostral VTA. **B.** Representative brightfield photomicrograph of CB₁R-IR (brown staining) in a coronal section of the rostral [-5.0mm Bregma] VTA (100x magnification). **C.** Representative brightfield photomicrograph of CB₁R-IR in the IF of the rostral VTA (200x magnification) and **D.**

High magnification (400x) image displaying a CB₁R-IR labeled cell in the IF; CB₁R-IR is dispersed throughout the cell body and in processes (arrowhead). **E.** Representative brightfield photomicrographs of CB₁R-IR in PBP nucleus of the rostral VTA (200x magnification). **F.** High magnification (400x) image displaying a CB₁R-IR labeled cell in the PBP; CB₁R-IR is dispersed throughout the cell body and in processes (arrowhead).

Figure 5.

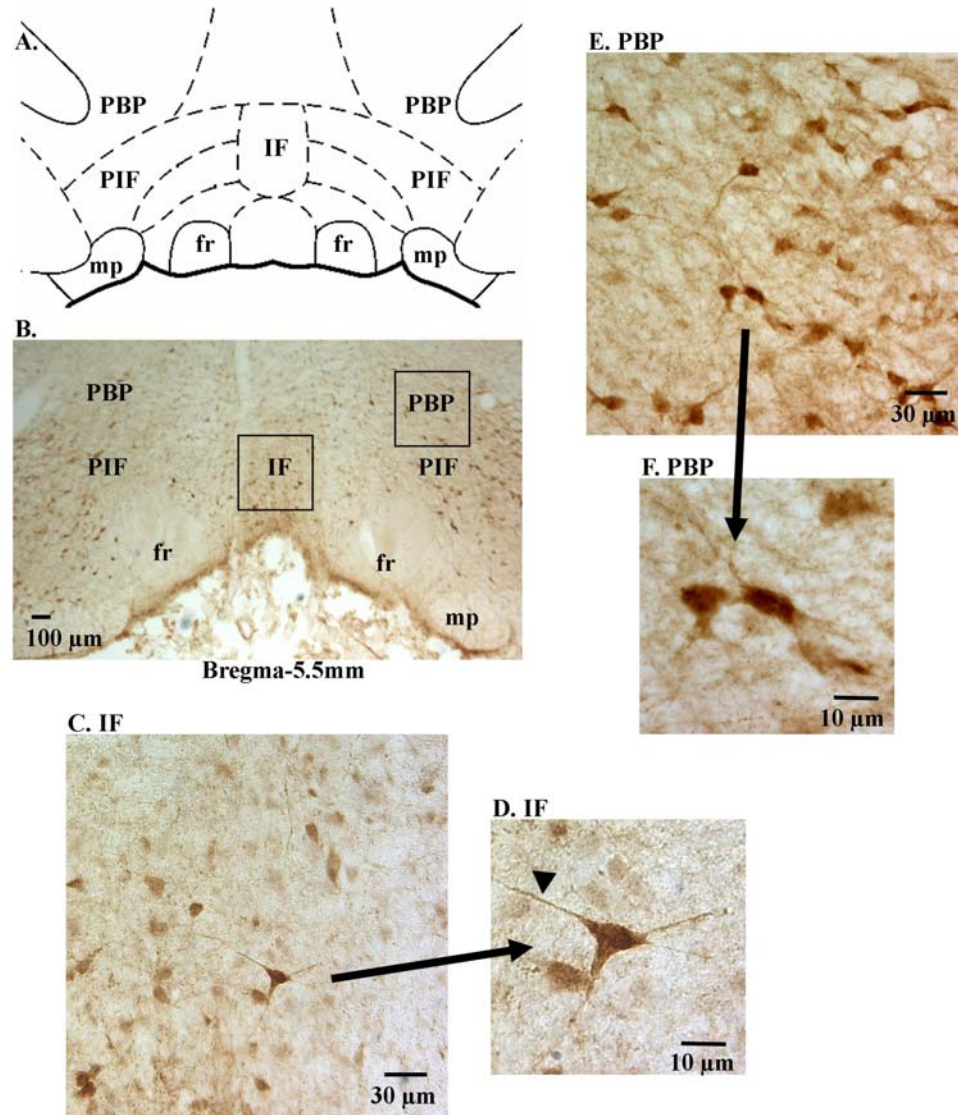


Figure 5. Middle VTA CB₁R-IR Expression

Schematic representation of the middle VTA at -5.5 mm Bregma (adapted from Paxinos and Watson, 2005). Landmark structures and subnuclei included: fasciculus retroflexus (fr), interfascicular nucleus (IF), parainterfascicular nucleus (PIF), parabrachial pigmented nucleus (PBP), and mammillary peduncle (mp) **A.** Representative atlas image of the middle VTA. **B.** Representative brightfield photomicrograph of CB₁R-IR (brown staining) in a coronal section of the middle [-5.5mm bregma] VTA (100x magnification). **C.** Representative brightfield photomicrograph of CB₁R-IR in the IF of the middle VTA

(200x magnification) and **D.** High magnification (400x) displaying a CB₁R-IR labeled cell; CB₁R-IR is dispersed throughout the cell body and in processes (arrowhead). **E.** Representative brightfield photomicrographs of CB₁R immunoreactivity in the PBP of the rostral VTA (200x magnification) and **F.** High magnification (400x) image displaying a CB₁R-IR labeled cell in the PBP; CB₁R-IR is dispersed throughout the cell body and in processes.

Distribution of VTA CB₁R-IR Positive Neurons

To enable comparisons across ROIs of different sizes, the density of cells normalized to area (cells/0.1 mm²) was calculated for each ROI. Significant differences in the expression of CB₁R-IR positive cells were observed throughout the VTA using a mixed model of statistical analysis. CB₁R-IR positive cells in the IF were the most densely packed of all subnuclei at all three levels of the VTA and the IF contained increasing numbers of labeled cells from rostral to caudal subnuclei (**Figure 7**). The number of cells per area in the middle IF was significantly higher than the number of cells per area in the rostral IF (* $p=0.0048$; **Figure 7**). The number of cells per area in the caudal IF was significantly higher than the number of cells per area in both the rostral and middle IF ($\#p<0.0001$; **Figure 7**). The number of cells per area in caudal PN was also significantly higher than the number of cells per area in both the rostral and middle PN ($\wedge p=0.010$; **Figure 7**), although this difference was markedly smaller than the increase detected in the IF. Thus, the density of cells normalized to area was the highest in the caudal IF compared to rostral and middle IF, as well as compared to all other subnuclei at the caudal level (**Figure 7**), despite the fact that the total number of cells counted in the ROI for the caudal IF was smaller relative to other caudal subnuclei.

A similar number of cells per area was observed in the rostral and middle PBP while the caudal PBP tended to contain a slightly higher number of cells per area ($p=0.0531$; **Figure 7**) compared to the rostral and middle PBP. The number of cells per area in the caudal PN was significantly higher than the number of cells per area in the middle PN (**Figure 7**; $p=0.001$). Conversely, the number of cells per area in the caudal PIF tended to be lower than the number of cells per area in the middle PIF ($p=0.1150$). Overall, with the exception of the PIF, increased numbers of cells per area were observed in all subnuclei in the rostrocaudal orientation.

Figure 6.

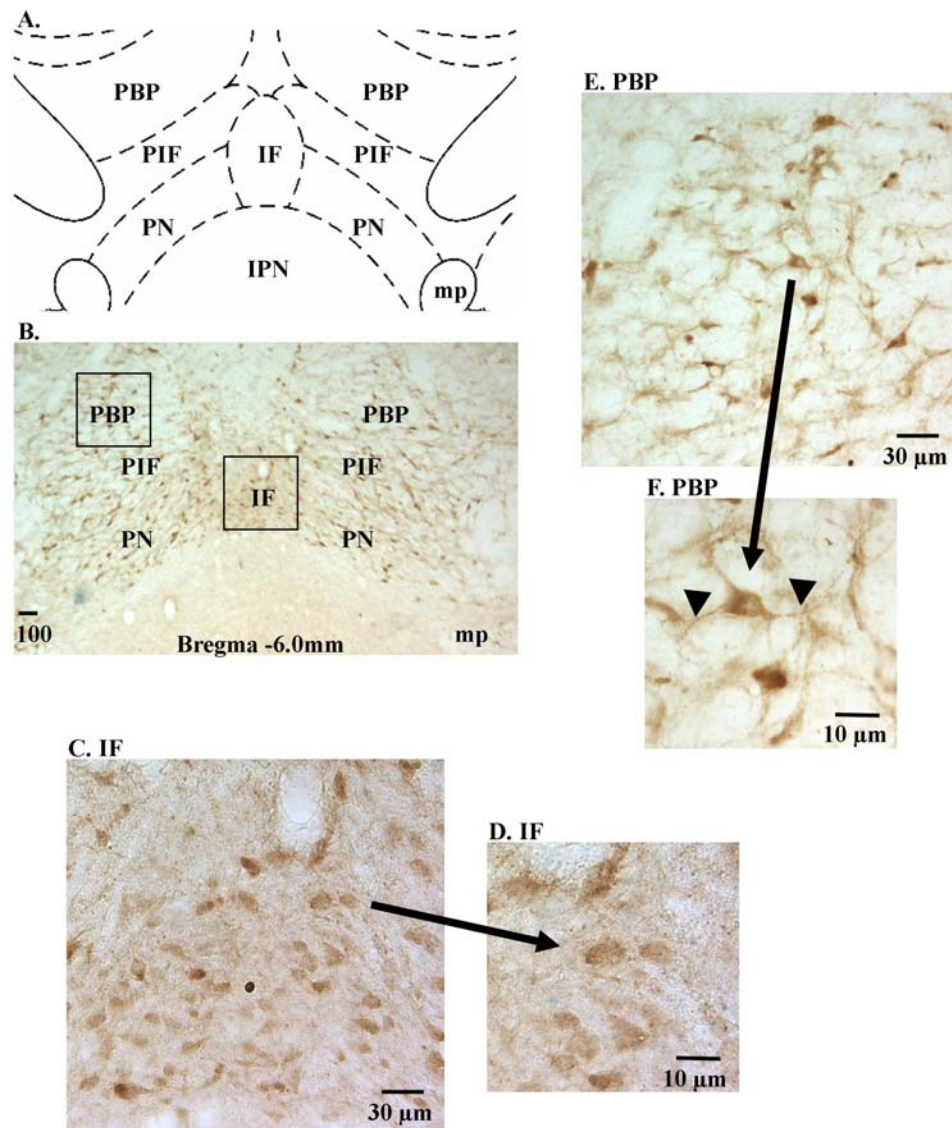


Figure 6. Caudal CB₁R-IR Expression

Schematic representation of the caudal VTA at -6.0 mm bregma. (adapted from Paxinos and Watson, 2005) Landmark structures and subnuclei included: fasciculus retroflexus (fr), interpeduncular nucleus (IPN), interfascicular nucleus (IF), parainterfascicular nucleus (PIF), parabrachial pigmented nucleus (PBP), and mammillary peduncle (mp). **A.** Representative atlas image of the caudal VTA. **B.** Representative brightfield photomicrograph of CB₁R-IR (brown staining) in a coronal section of the caudal [-6.0mm bregma] VTA (100x magnification). **C.** Representative brightfield photomicrograph of

CB₁R-IR in the IF of the caudal VTA (200x magnification) and **D.** High magnification (400x) displaying a CB₁R-IR labeled cell; CB₁R-IR is dispersed throughout the cell body and in processes. **E.** Representative brightfield photomicrographs of CB₁R immunoreactivity in PBP of the caudal VTA (200x magnification) and **F.** High magnification (400x) image displaying a CB₁R-IR labeled cell in the PBP; CB₁R-IR is dispersed throughout the cell body and in processes (arrowheads).

Figure 7.

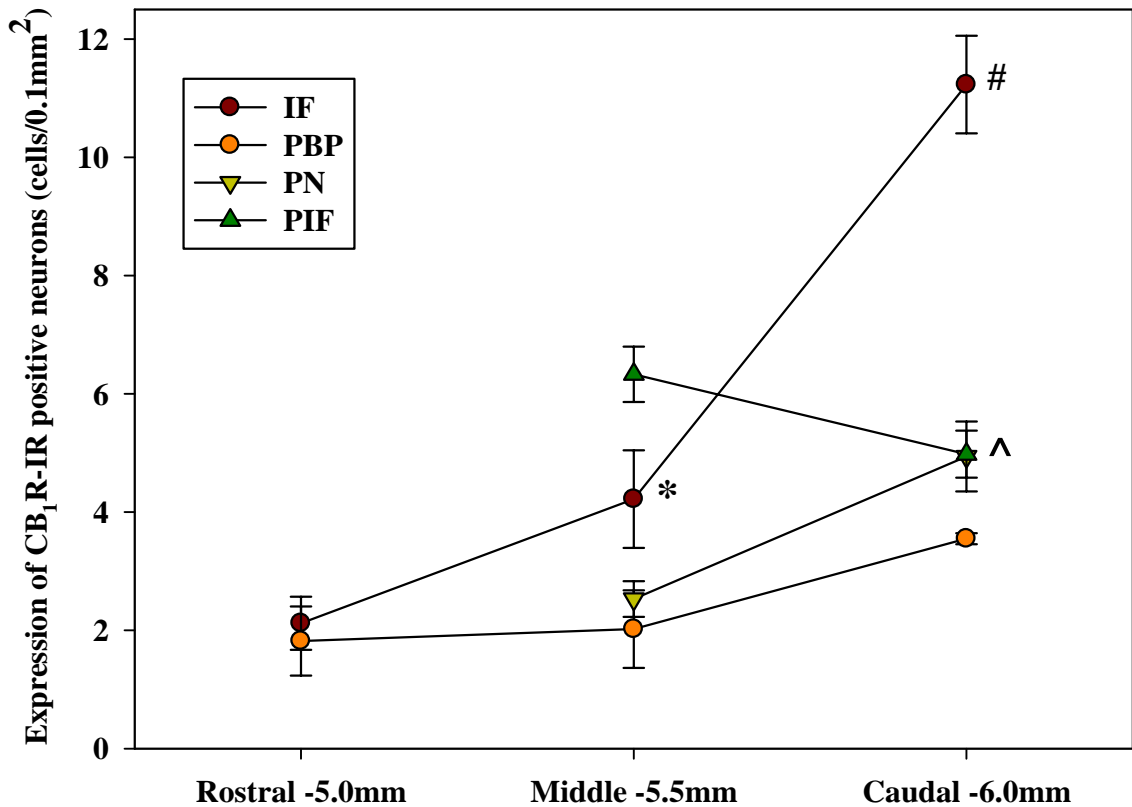


Figure 7. VTA CB₁R-IR Expression

The expression of VTA CB₁R-IR positive cells (cells/100 μ m²) within each subnucleus across the rostrocaudal extent of the VTA. Statistical comparisons are made between rostrocaudal levels of each subnucleus. Means (\pm SEM) described are of 3 images per 3 sections per area analyzed. Significant differences are observed between the caudal IF compared with the middle IF and the rostral IF (# $p < 0.05$), the middle IF compared with the rostral IF and the caudal IF (* $p < 0.05$), and the caudal PN compared with the middle PN (^ $p < 0.05$).

DISCUSSION

The present study is the first to demonstrate RNA specific for the CB₁R in the VTA as well as thoroughly quantify the localization of the CB₁R protein within the VTA. A PCR analysis of cDNA generated from RNA isolated from rat VTA tissue sections confirmed the presence of CB₁R specific RNA; previous reports had not included the VTA in their studies of localization of CB₁R RNA expression in rat brain (Gonzalez et al., 2005; Hurley et al., 2003; Romero et al., 2000; Silverdale et al., 2001). The CB₁R protein was expressed throughout entire cells and within fiber-like structures in component subnuclei of the VTA. Low-to-moderate numbers relative to other VTA levels of CB₁R-IR positive cells were observed in subnuclei represented at rostral and middle levels, while moderate-to-high numbers relative to other VTA levels of CB₁R-IR positive cells were found in the caudal VTA. The caudal IF contained the highest density of cells that expressed the CB₁R in the entire VTA. The present findings provide molecular evidence in support of previous immunohistochemical (Wenger et al., 2003), radiolabeled-agonist binding (Herkenham et al., 1991b), electrophysiological (French et al., 1997; Gessa et al., 1998; Melis et al., 2004; Szabo et al., 2002) and behavioral studies (Gardner, 2002; Zangen et al., 2006) to support the localization of CB₁R to neurons in the VTA.

The VTA is the origin of the mesocorticoaccumbens DA pathway and DA-containing cell bodies originating in the VTA terminate in the NAc and other brain regions to comprise a circuit important in reward, motivation, and emotion (German and Manaye, 1993b; Kalivas and Nakamura, 1999; Pierce and Kumaresan, 2006; Wise, 2005). In the present study, the highest expression of the CB₁R-IR was localized to the caudal extent of all subnuclei studied (IF, PBP, PN, PIF). This observation is in keeping with recent studies to suggest that the population of CB₁R found in the posterior VTA appears to be important in the expression of behaviors evoked by cannabinoids. For example, microinfusion of Δ^9 -THC into the posterior (but not anterior) VTA evoked hyperactivity, a conditioned place preference and self-administration, all of which were attenuated by the cannabinoid antagonist SR141716a (Zangen et al., 2006). Furthermore, recent reports indicate that systemically-administered cannabinoids differentially alters the expression levels of several cellular markers within VTA subnuclei. For example, chronic Δ^9 -THC administration preferentially induced brain derived neurotrophic factor (BDNF)

expression in the caudal VTA (4-fold change) compared to the rostral VTA (1.7-fold change) (Butovsky et al., 2005). Thus, taken together, these data support the hypothesis that the CB₁R plays an important modulatory role in behavior which is functionally dependent upon its regional expression in the VTA.

Of particular interest is the relatively high level of CB₁R expression in the caudal IF compared to that of other VTA subnuclei. Although not previously considered to be the case (Phillipson and Griffith, 1980), the IF is now categorized as a component nucleus of the VTA given the predominance of DA-containing neurons in the IF as well as the topography of its efferents (Swanson, 1982c). The IF projects bilaterally to the limbic cortex, NAc, the amygdala and lateral septum, with a preponderance of these projections arising from DA neurons in the IF; non-DA neurons of the IF contribute predominantly to the significant projection of the IF to the lateral habenula (Swanson, 1982c). While knowledge of specific afferent innervation of the IF is limited, the overall topography of innervation of the VTA is now considered to a complex “linked network” (Geisler and Zahm, 2005) which includes descending projections from the PFC, NAc (shell), lateral septum, ventral pallidum, and ascending projections from the dorsal raphe, medial and periaqueductal grey, to name just a few of the interconnected nuclei (Geisler and Zahm, 2005). While these interconnections suggest that the IF may play an important role in neurobiology, the actual functional role of the IF is obscure. Thus, the specific implications of CB₁R localization to the IF are difficult to ascertain. It is possible that the IF contributes to the behavioral effects of cannabinoids delivered directly to the posterior VTA (Zangen et al., 2006), but the independent role of CB₁R in the IF to control behaviors driven by cannabinoids will be difficult to establish because the small size of the nucleus is not conducive to intracranial microinfusion analyses.

The CB₁R-IR was detected in cellular- and fiber-like structures in numerous brain areas that were previously reported to contain populations of CB₁R such as the NAc shell, dorsal raphe nucleus, PFC and medial septal nucleus (Herkenham et al., 1991b; Tsou et al., 1998) by immunohistochemistry. Interestingly, near uniform staining of a cell with a receptor-targeted antibody, such as the CB₁R, has been suggested to represent the detection of the receptor protein inside the cell in an inactive form, as is either newly synthesized or degrading state (Julian et al., 2003). Thus, some of the staining detected throughout entire cells in the VTA may therefore indicate populations of CB₁R in the

VTA are in their inactive form, located inside the cell and therefore potentially elusive to previous staining protocols. As the present studies utilized a detergent-based immunohistochemical tissue processing protocol, the permeability of cells to the primary and secondary antibodies was more likely to enhance access of antibodies to the internal compartments of cells in the tissue sections (Wikstrom et al., 1987).

Our demonstration of VTA CB₁R-IR expressed throughout entire cells as well as along cellular processes indicates that CB₁R populations are not as discretely localized as some current mechanistic studies have hypothesized. Although there is strong electrophysiological evidence for presynaptic localization of CB₁R on GABA terminals (Szabo et al., 2002) as well as glutamate terminals in the VTA (Melis et al., 2004), there is also a growing body of evidence which describes both K⁺-mediated (Kirby et al., 2000) and Ca⁺-mediated (Endoh, 2006) postsynaptic effects of cannabinoid agonists in neurons, effects which are blocked by cannabinoid antagonists. For example, the cannabinoid agonist WIN 55,212-2 induced a K⁺-dependent membrane hyperpolarization in neurons recorded in hippocampal slice preparations which were blocked with the antagonist SR141716a (Kirby et al., 2000). Additionally, application of WIN55,212 to neurons in nucleus tractus solitarius inhibited postsynaptic I_{Ba} Ca⁺ currents that were blocked with the cannabinoid antagonist AM281 (Endoh, 2006). The application of the cannabinoid agonists methanadamide or WIN55,212 also decreased voltage dependent K⁺ I_M in hippocampal CA1 neurons, an effect blocked by application of SR141716a (Schweitzer, 2000). Furthermore, WIN55,212 reduced fast e.p.s.p.s both pre- and postsynaptically when applied to myenteric neurons (Lopez-Redondo et al., 1997). These data are backed by immunohistochemical and electron microscopy analyses which show CB₁R protein expression within cytoplasm and plasma membranes in somatodendritic profiles as well as cell bodies of NAc medium-sized spiny neurons (Pickel et al., 2004), caudate putamen neurons (Rodriguez et al., 2001) and neurons in dorsal horn of the spinal cord (Salio et al., 2002). Additionally, *in vivo* binding studies demonstrated receptor binding (50%) after extensive rhizotomy and complete deafferentation in spinal cord (Hohmann et al., 1999). Thus, the CB₁R expression described in the VTA most likely represents a combination of pre- and postsynaptically localized CB₁R populations.

The demonstration that the CB₁R is localized to VTA cells is predicated upon the use of an anti-CB₁R antibody validated to be specific. We demonstrated that RNA for

CB₁R can be amplified from samples of whole VTA indicating the potential for the intra-VTA production of CB₁R protein, which is in line with our demonstration of CB₁R protein expression throughout the VTA. Furthermore, the anti-CB₁R antibody employed here has been independently authenticated to selectively stain CB₁R protein in immunohistochemical studies of cultured cells and brain tissue (Ashton et al., 2004a; Ashton et al., 2004d; Ashton et al., 2004c; Ashton et al., 2004b; Ashton et al., 2006a; Ashton et al., 2006b; Jiang et al., 2005; Smith et al., 2006; Vallano et al., 2006). Detection of an appropriately-sized (60 kDa) band for CB₁R protein was also obtained with this antibody in immunoblot analyses of cells that have been characterized to express CB₁R mRNA and respond to a selective CB₁R agonist (HU-210); both immunostaining and immunoblot detection were eliminated with antisera preabsorption (Jiang et al., 2005). Thus, RNA and protein analysis conducted here further the specificity of this antibody and instills confidence in the conclusion that the CB₁R is localized to the VTA.

The knowledge of CB₁R distribution within VTA gained from the present study provides an important foundation for the development of future studies to further delineate the actions and/or role of VTA CB₁R in the neurobiological mechanisms of marijuana abuse. The present study establishes CB₁R-IR and RNA within the VTA at highest concentrations in the caudal VTA. In addition, the present findings provide evidence in support of a previous immunohistochemical study (Wenger et al., 2003), electrophysiological studies (French et al., 1997; Gessa et al., 1998; Melis et al., 2004; Szabo et al., 2002) and behavioral studies (Zangen et al., 2006) which have demonstrated the expression of CB₁R in the VTA. These data establish regio-specificity through which cannabinoids may modulate the mesoaccumbens pathway to evoke aspects of the rewarding potential of cannabinoids.

CHAPTER 3

Selective Ablation of Neurons Expressing μ -Opioid Receptors in the Ventral Tegmental Area: Increased Spontaneous Locomotor Activity and Cocaine Hyperactivity

ABSTRACT

Gamma-aminobutyric (GABA) acid neurons of the VTA function as important regulators of mesoaccumbens DA circuits which contribute importantly to the generation of behaviors induced for abused drugs, best described for the psychostimulant cocaine. A subset of these GABA-containing neurons possess μ -opioid receptors and are sensitive to the neurotoxic actions of the ribosome-inactivating molecule saporin conjugated to the μ -opioid agonist dermorphin (dermorphin-saporin; DS). We utilized DS to test the hypothesis that ablation of GABA-containing neurons in the VTA will result in disinhibition of motor activity and potentiation of cocaine-induced hyperactivity. Rats ($n=16/\text{group}$) were bilaterally microinfused with DS (1.0 or 2.0 pmol) or blank-saporin (BS, 200 nl/side) into the VTA. Seven days later, DS-treated rats exhibited significantly elevated baseline motility compared to BS-treated rats ($p < 0.05$); this elevated motility disappeared by day 14 in rats pretreated for the low dose of DS (1.0 pmol) and was still evident on day 14 after pretreatment with the high dose of DS (2.0 pmol). Furthermore, seven days following DS pretreatment at the lowest dose (1.0 pmol), cocaine-induced (10 mg/kg, IP) hyperactivity was observed, which appeared additive with an elevated baseline. At 14 days following DS lesion, animals returned to normalized baseline motor activity but maintained elevated cocaine-induced hyperactivity. A selective loss of GABA-containing neurons in the VTA at day 14 after pretreatment was established by significantly reduced expression of mRNA for both glutamic acid decarboxylase 67 (GAD-67) and μ -opioid receptor but not; tyrosine hydroxylase (a marker for DA-containing neurons) in the VTA. Thus, selective losses of GABA-containing neurons caused administration of DS into the VTA led to disinhibition of motor activity and potentiated cocaine hyperactivity. These data reinforce the hypothesis that GABA-containing neurons of the VTA are important inhibitory modulators of spontaneous as well as psychostimulant-induced motor activity.

INTRODUCTION

Mesocorticoaccumbens dopamine (DA) circuits which originate in the ventral tegmental area (VTA) and project to various brain nuclei including the nucleus accumbens (NAc) and the prefrontal cortex (PFC) are involved in mediating both spontaneous motility and stimulant-induced motor hyperactivity (Creese and Iversen, 1973; Kelly and Iversen, 1975; Pierce and Kumaresan, 2006). This same pathway is important in the physiology of the rewarding (Koob and Nestler, 1997; Wise, 1998) and reinforcing effects of drugs of abuse (Di Chiara and Imperato, 1988a; Spanagel and Weiss, 1999). The ability of psychostimulants to elicit locomotor hyperactivity correlates with their ability to increase DA efflux in the NAc, the terminal region of the DA mesoaccumbens or “reward” pathway (Erinoff and Brown, 1994). Therefore, motor activity correlates as an indirect measure of activation of the “reward” pathway (Wise and Bozarth, 1987). Regulation of the pathway at the level of VTA DA signaling is driven by multiple afferent input systems (Kalivas and Nakamura, 1999). A key regulatory component is the inhibitory GABA input from local GABA-containing interneurons in the VTA and from GABA-containing projection neurons that innervate the VTA (Mathon et al., 2003; White, 1996). This GABA innervation at the level of the VTA plays an important role in modulation of the mesoaccumbens pathway (Grubb et al., 2002; Kelly et al., 1977).

Afferent GABA input modulates the cell firing of DA-containing neurons (Korotkova et al., 2004). The VTA GABA-containing neurons themselves are under the control of several neurotransmitter systems. Immunohistochemical and electrophysiological studies suggest important afferent control of GABA-containing interneurons by GABA receptors (Klitenick et al., 1992), CB₁R (as we have shown in Chapter 2), opioid receptors (Klitenick and Wirtshafter, 1995), as well as other receptor systems. Key inhibitory GABA afferents modulate cell firing of DA-containing neurons through GABA receptor systems and GABA-containing neurons are known to express high levels of μ -opioid receptor mRNA and protein (Mansour et al., 1995). The μ -opioid receptor protein and mRNA have been localized to GABA-containing neurons within the VTA (Garzon and Pickel, 2001; Garzon and Pickel, 2002; Nikulina et al., 1999). Application of opiate agonists induced membrane hyperpolarization of GABA-containing

neurons in the VTA, thus dampening their spontaneous activity which results in a loss of inhibitory control (disinhibition) of DA-containing neurons (De Vries and Shippenberg, 2002; Johnson and North, 1992b). In keeping with this hypothesis, microiontophoretic application of the μ -opioid receptor agonist morphine into the VTA increased firing of DA-containing neurons which is blocked by the opioid antagonist naloxone (Gysling and Wang, 1983; Matthews and German, 1984). Additionally, microiontophoretic application of the selective μ -receptor agonist DAMGO into the VTA increased firing of DA-containing neurons (Johnson and North, 1992a). Furthermore, morphine application also decreased GABA release in an *in vitro* VTA preparation (Bergevin et al., 2002) presumably accounting for the increased cell firing of DA-containing neurons. Thus, the μ -opioid receptor is a key inhibitory modulator of GABA afferents in the VTA.

A subset of VTA GABA-containing neurons express μ -opioid receptors and therefore are sensitive to the neurotoxic actions of saporin conjugated to the μ -opioid agonist dermorphin [dermorphin-saporin (DS)]. Saporin is a plant-derived neurotoxin which kills neurons via a ribosomal inactivation mechanism (Advanced Targeting Systems, San Diego CA). When conjugated to dermorphin, this complex (DS) binds to μ -opioid receptors allowing specific uptake of the toxin into the cell (Wiley, 1992). This targeted ablation of cells that express the μ -opioid receptor has been demonstrated in numerous brain areas, including the brainstem (Porreca et al., 2001), medulla (Burgess et al., 2002), and striatum (Tokuno et al., 2002). The doses of DS chosen for the present study (1 and 2 pmol/200nl/side) were based on the published literature of neuronal ablation leading to a robust behavioral response (Porreca et al., 2001) in which DS pretreatment was capable of generating 59-78% decrements in the maximal possible sensitivity to experimental neuropathic pain (Porreca et al., 2001). The ability to selectively ablate VTA GABA-containing neurons which express μ -opioid receptors using DS allows the examination of the role of this population of VTA GABA-containing neurons in the modulation of behavior including motor activity.

The goal of the present experiment was to test the hypothesis that the loss of VTA GABA-containing neurons consequent to DS pretreatment would increase basal spontaneous locomotor activity and/or cocaine-induced hyperactivity. We chose to analyze locomotor activity induced by cocaine because the behavioral effects of this locomotor stimulant are mediated in large part via the mesoaccumbens pathway. The

primary action of cocaine is to block the DA transporter (Koe, 1976) and thereby increase NAc DA efflux and subsequently the generation of locomotor hyperactivity (Di Chiara and Imperato, 1988b). The GABA inhibition of VTA DA-containing neurons modulates basal locomotor activity and thus may also modulate motor hyperactivity induced by cocaine administration. Therefore, the selective loss of GABA-containing neurons in the VTA would be expected to increase basal activity and enhance cocaine-induced hyperactivity. We determined the degree of loss of GABA-containing neurons after DS pretreatment by measurement of RNA levels for the μ -opioid receptor, gamma-aminobutyric acid 67 (GAD-67, a marker for GABA-containing neurons) and tyrosine hydroxylase (TH, a marker for DA-containing neurons) in the VTA. Immunohistochemistry was used to visualize expression for μ -opioid receptor, GAD-67 and TH in the VTA of control and treated rats. We demonstrated increased basal as well as cocaine-evoked locomotor activity after DS pretreatment and therefore these studies shed light on the involvement of VTA GABA-containing neurons in the generation of spontaneous activity as well as cocaine-induced hyperactivity and provide important evidence regarding the inhibitory control of GABA-containing neurons over DA-containing neurons of the VTA.

MATERIALS AND METHODS

Animals

Male Sprague-Dawley rats (n=144) Harlan Sprague-Dawley, Inc., Indianapolis, IN) weighed 275-300 g at the beginning of the study. The rats were single-housed in standard plastic rodent cages in a temperature (21-23°C) and humidity (55-65%) controlled environment under a 12-h light/dark cycle (lights on 0700 h). Animals were acclimated to the colony for at least one week prior to the start of experimental sessions. Experiments were conducted during the light phase (1200-1800 h) and were conducted in accordance with the National Institutes of Health *Guide for the Care and Use of Laboratory Animals* and with approval from the Institutional Animal Care and Use Committee.

Drugs

The conjugated toxin dermorphin-saporin (DS) and blank-saporin (BS; Advanced Targeting Systems, San Diego, CA) the toxin conjugated to a blank sequence with no known affinity to any known receptor were suspended in filtered sterile saline. Cocaine (National Institutes on Drug Abuse, Research Triangle Park, NC, USA) was dissolved in 0.9% NaCl.

Dermorphin-Saporin Pretreatment Protocol

Rats were anesthetized (IM) with a cocktail of 43 mg/kg of ketamine, 8.6 mg/kg of xylazine and 1.5 mg/kg of acepromazine in physiological saline (0.9% NaCl), then placed in a Kopf rat stereotaxic apparatus (David Kopf Instruments, Tujunga, CA) with the upper incisor bar at -3.8 mm below the interaural line. Two Hamilton microsyringes (5 μ l, Hamilton, Reno, NV) were lowered bilaterally into the VTA at a 6° angle from the midsagittal plane in relation to bregma [anteroposterior -6.0 mm; mediolateral +1.4 mm; dorsoventral -8.0 mm from skull (Paxinos and Watson, 2005)]. Infusion of BS (1 pmol/200nl/side) or DS (1 or 2 pmol/200nl/side) into the VTA (n=8 rats / group) was accomplished using the UMP II infusion pump (WPI, Sarasota, FL) set at an infusion rate of 18 nl/min; the infusion lasted for 11.1 min. Following infusion, the needles remained in place for 10 min before withdrawal from the brain and wound closure with sutures. Rats received a single injection (IM) of 300,000 U of sodium ampicillin after surgery, a single injection (SC) of 1 ml of filtered saline, and were allowed six days to recover, during which time they were handled and weighed daily.

Measurement of Locomotor Activity

All rats were habituated to the test environment for 3 hr per day on each of the 2 days prior to the start of the experiment and for 1 hr prior on test days. Activity was monitored and quantified under low light conditions utilizing a modified open field system (San Diego Instruments, San Diego, CA) housed within sound-attenuated chambers. Each enclosure consisted of a clear Plexiglas chamber (40 x 40 x 40 cm). A 4x4 photobeam matrix was located 4 cm above the cage floor with beams spaced at 8 cm intervals on the x and y planes. The interruption of two consecutive photobeams resulted

in a count of “ambulation” by the control software (Photobeam Activity Software, San Diego Instruments).

Experiment 1

Basal locomotor activity was assessed in response to pretreatment the BS, DS1, or DS2 (initial n=96, total) to test the hypothesis that loss of GABA-containing neurons in the VTA would modulate locomotor activity. Following recovery from surgery (day 7 or day 14, n=16 per group), animals were placed into the locomotor chamber for 1 hr. At the termination of the behavioral experiment, each group of rats was split into two separate groups, and tissue was extracted for quantitative rt-PCR analysis (n=8) and immunohistochemical assay (n=8). Locomotor activity data are presented as mean ambulation counts (\pm SEM) totaled for the 60 min observation period. Because group comparisons were specifically defined prior to the start of the experiment, planned comparisons were conducted in lieu of an overall F test in a multifactorial ANOVA; this statistical analysis has been supported in a number of statistical tests (Keppel, 1973). Thus, each experiment was subjected to a one-way ANOVA was used to compare pretreatment groups followed by planned, pairwise comparisons of means made with the Dunnett’s test (SAS for Windows, Version 8.1). Mean total ambulation was also divided into separate 5-min time bins and analyzed with a two-way ANOVA with time as a repeated measures factor; preplanned comparisons were made by using Fisher’s Least Significant Difference (LSD) test. All comparisons were conducted with an experiment wise error rate of $\alpha = 0.05$.

Experiment 2

To test the hypothesis that loss of GABA-containing neurons in the VTA would modulate basal and/or cocaine-induced hyperactivity. Locomotor activity was assessed in response to cocaine administration (initial n=48, total), 7 or 14 days after pretreatment the DS (1pmol/200nl/side; n=12) or BS (n=12). Following recovery from surgery (day 7 or day 14, n=12 per group), animals were injected with saline (1 ml/kg, IP) and placed into the locomotor chamber for 1 hr. At the end of 1 hr, rats were removed from the activity monitor briefly and injected with cocaine (10 mg/kg, IP) and returned to the locomotor monitor for 1 hr. At the termination of the behavioral assess rats were sacrificed.

Locomotor activity data are presented as mean ambulation counts (\pm SEM) totaled for the 60 min observation period. The experiment was subjected to a two-way ANOVA with the two levels of pretreatment (DS or BS) and treatment (saline or cocaine). Timecourse data were broken down and a three-way ANOVA was used with two levels of pretreatment (DS or BS) and treatment (saline or cocaine) with time (0-60 min) interactions. Preplanned comparisons between treatment groups were determined at each 5-min time point using a one-way ANOVA. All comparisons were conducted with an experiment wise error rate of $\alpha = 0.05$.

RNA Extraction

Seven or 14 days post-surgery, animals pretreated with either DS or BS (initial $n=8$ /group) were euthanized and tissue from the VTA was dissected on a cool tray (4°C) and stored in *RNAlater* (Ambion, Austin, TX) at -70°C for subsequent RNA extraction. RNA was prepared from brain tissue lysate using the *RNAqueous* kit (Ambion). Samples were treated with Turbo DNase (Ambion) in order to avoid chromosomal DNA contamination. The final RNA concentration was determined by absorbance at 260 nm.

Taqman Quantitative Realtime Reverse Transcription PCR (qRT-PCR)

Reverse transcription was performed on $1.0\ \mu\text{g}$ RNA using the TaqMan[®] Reverse Transcription Kit (Applied Biosystems, Inc., Foster City, CA) with random hexamer primers according to the manufacturer's directions. The resultant cDNA was quantified by TaqMan[®] real-time PCR assays (Applied Biosystems) using an ABI PRISM[®] 7700 Sequence Detection System (Applied Biosystems). GAD-67 primers were designed with Primer 3 (Whitehead Institute for Biomedical Research) using stringent parameters to reduce primer dimerization and to minimize the difference between melting temperatures (T_m) of primers. Sense (5' GGC TGA TGT GGA AAG CAAG 3') and antisense (5' TCG GAG GCT TTG TGG TAT GT 3') primers amplified a 176 bp region between bases 1575 and 1750 (Accession # M76177). Primers were first tested by using conventional PCR: products were characterized by agarose gel electrophoresis for the correct size and for the absence of non-specific bands, then by direct DNA sequencing (Sealy Center for Molecular Science, University of Texas Medical Branch, Galveston, TX) to confirm the identity of the amplicon.

Two predesigned rat TaqMan® gene expression assays were used to quantify rat tyrosine hydroxylase (Rn_00562500_m1) and rat μ -opioid receptor (Rn_0056144_m1) gene expression (Applied Biosystems, Foster City, CA). The qRT-PCR amplification program consisted of a 95°C 10 min activation step followed by 40 cycles of denaturation (95°C for 15 s), annealing (60°C for 30 s), and elongation (72°C for 30 s). All sample reactions were run in triplicate and data from each sample were normalized to cyclophilin (sense primer, 5' TGT GCC AGG GTG GTG ACT T 3'; antisense primer, 5' TCA AAT TTC TCT CCG TAG ATG GAC TT 3'; probe [FAM] ACA CGC CAT AAT GGC ACT GGT GG [DTAM]).

The relative quantification method was used to compare differences between samples (Livak and Schmittgen, 2001). The crossing threshold (Ct) is defined as the cycle at which sample fluorescence crosses a threshold set above background noise and within the logarithmic portion of the amplification curve. The difference in crossing thresholds (Δ Ct) was calculated for each gene being studied: Δ Ct = Ct (gene of interest) – Ct (cyclophilin) for each sample. Mean Δ Ct \pm SEM was determined for each group. The magnitude of the differences between groups was calculated as: $\Delta\Delta$ Ct = Δ Ct(control) - Δ Ct(test); fold increase (or decrease) was estimated by $2^{-\Delta\Delta$ Ct}.

Statistical Analyses for Quantitative PCR

The relative mRNA content in each sample was expressed as $\Delta\Delta$ C_T of the mean of treatment group and each individual reaction was processed in triplicate. Data are represented as mean $\Delta\Delta$ C_T \pm SEM. The effect of pretreatment with DS or BS was assessed using the non-parametric Wilcoxon (Kruskal-Wallis) test to determine whether differences between groups were significant; this type statistical analysis design is supported in a number of statistical models for quantification qRT-PCR (Fu et al., 2006; Yuan et al., 2006). All statistical analyses were conducted with an experimentwise error rate $\alpha = 0.05$.

Immunohistochemistry

To visualize expression of protein, rats (initial n=8/group) were deeply anesthetized with pentobarbital (80 mg/kg) and perfused transcardially with phosphate buffered saline (PBS) followed by 3% buffered paraformaldehyde. After brain removal

and post-fixation (2 hr), brains were transferred to a 30% sucrose solution (4°C, 2 days), then rapidly frozen with crushed dry ice and stored at -70°C until sectioning. Consecutive sections (35 µm) containing the lesioned VTA were taken using a cryostat (Leica CM1850) at -20°C. Standard procedures were employed for immunodetection (Frankel and Cunningham, 2002). Briefly, following extensive washes, non-specific binding was blocked by 0.4% Triton X-100 in PBS containing 1.5% normal goat serum (Vector Laboratories, Burlingame, CA) 1 hr, then tissue sections were incubated in primary antibody (2 days, 4°C). Three primary antibodies were used in consecutive sections for each brain processed: anti-µ-opioid receptor (cat. # RA10104, Neuromics, Bloomington, MN), anti-TH (cat. # 22941, Immunostar, Hudson, WI) and anti-GAD-67 (cat. # H-101, Santa Cruz Biotechnology, Santa Cruz, CA). The rabbit anti-µ-opioid receptor antibody has been validated (Kim et al., 2006) and utilized in several prior immunohistochemical studies (Chen and Pan, 2006; Luo et al., 2005). The mouse anti-tyrosine-hydroxylase antibody (Huang et al., 2005; Kim et al., 2005) and the rabbit anti-GAD-67 antibody have been utilized in several prior studies for immunohistochemical (Akema et al., 2005; Falk et al., 2006; Majak and Pitkanen, 2003) and Western blot analyses (Akema et al., 2005; Sanchez et al., 2006). Following extensive washing with PBS, sections were incubated in a secondary antibody solution (biotinylated goat anti-rabbit or anti-mouse IgG; Vector) for 1 h, then avidin/biotin-horseradish peroxidase complex (ABC; Vectastain Elite kit; Vector Laboratories; Burlingame, CA) for 1 h. The sections were rinsed 3x in Tris buffer (pH 7.6) followed by incubation in diaminobenzidine (0.5 mg/ml) with 0.005% H₂O₂. The chromagen reaction was terminated by placing the sections in PBS. Sections were placed in a 0.1% Drefits solution and mounted onto slides previously coated with gelatin chrom alum. DPX mounting medium (Fisher Scientific, Houston, TX) was used to coverslip the slides. Images of stained tissue sections were captured with a system consisting of an Olympus B51 microscope and a Professional Hamamatsu digital camera (Hamamatsu Digital Camera C4742-95, Japan) and analyzed with Simple PCI (6.0, Compix Inc., Cranberry Township, PA) imaging software.

RESULTS

Effects of Intra-VTA Microinjection of Dermorphin-Saporin on Basal Activity

The mean total ambulation counts/60 min (\pm SEM) was assessed 7 days (**Figure 8**) following pretreatment with BS ($n = 9$) or [DS 1 ($n = 10$) or DS 2 ($n = 10$); 1.0 or 2.0 pmol/200nl/side, experiment 1]. A main effect of pretreatment with DS ($F_{2,28} = 16.47$; $p = 0<.0001$, **Figure 8**) on ambulation counts was observed on day 7. Preplanned comparisons indicated that mean total ambulation counts were significantly greater in animals treated with either dose of DS compared to BS animals ($p < 0.05$). Administration of intra-VTA DS did not appear to induce overt impairments in balance, gait, or ambulation (data not shown).

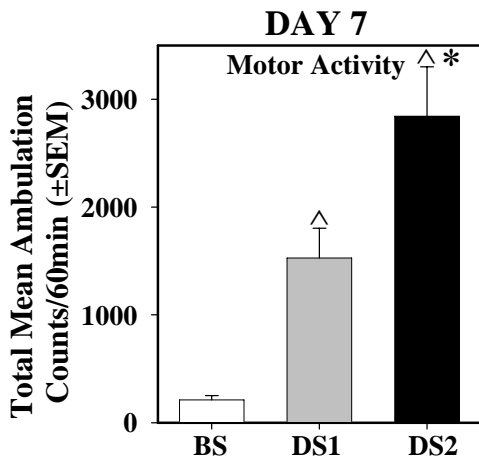


Figure 8. Intra-VTA Dermorphin-Saporin (Day 7 pretreatment) Increases Mean Total Ambulation

Effects of intra-VTA pretreatment with the μ -opioid receptor specific toxin dermorphin-saporin (DS) on mean total ambulation counts (\pm SEM) for rats pretreated 7 days previously with BS control (BS; $n=8$) or DS (DS1 or DS2; 1 or 2 pmol/200nl/side; $n=8$).

A two-way ANOVA indicated a main effect of pretreatment ($F_{2,22} = 33.97$, $p<0.0001$), a main effect of time ($F_{2,22} = 4.78$, $p<0.0001$, experiment 1), and a significant treatment x time interaction for mean total ambulation ($F_{2,22} = 1.73$, $p<0.05$, **Figure 9**). Examination of the timecourse using individual one-way ANOVA and Fisher's LSD test indicated significant elevations of ambulatory motor activity in both groups of DS-treated rats compared to control rats ($p<0.05$).

Figure 9.

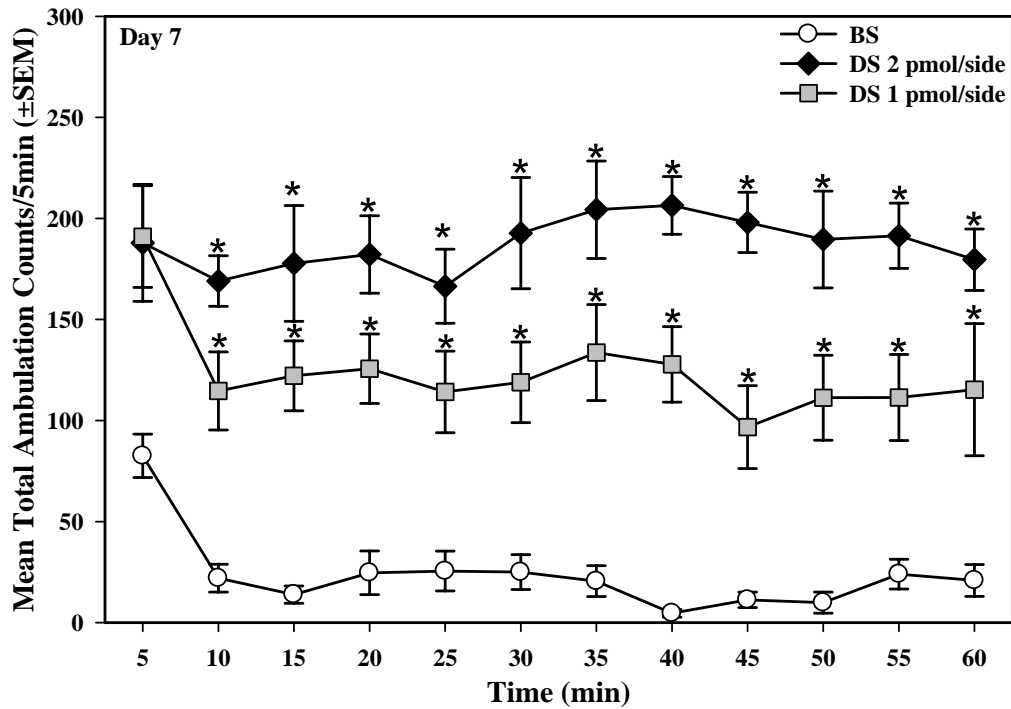


Figure 9. Elevated Ambulation at Day 7 after Intra-VTA Dermorphin-Saporin

Effects of intra-VTA pretreatment of the μ -opioid receptor specific toxin dermorphin-saporin (DS) on the mean total ambulation in 5 min time bins (\pm SEM) for rats previously pretreated with BS control (BS; n=9) or DS (DS1 or DS2; 1 or 2 pmol/200nl/side; n=10) 7 days after pretreatment. * Ambulation levels that were significantly different from BS at the corresponding time point based upon Fisher's Least Significant Difference test.

Mean total ambulation counts/60 min (\pm SEM) were assessed 14 days (**Figure 10**, experiment 1) following pretreatment with BS (n = 11) or [DS 1 (n = 11) or DS 2 (n = 11); 1.0 or 2.0 pmol/200nl/side, experiment 1]. A main effect of pretreatment ($F_{2,31} = 6.79$; $p < 0.05$) on ambulation counts was observed on day 14. Preplanned comparisons indicated that mean total ambulation counts were significantly greater in animals pretreated with the higher dose of DS (2.0 pmol/200nl/side) compared to BS-treated control animals ($p < 0.05$).

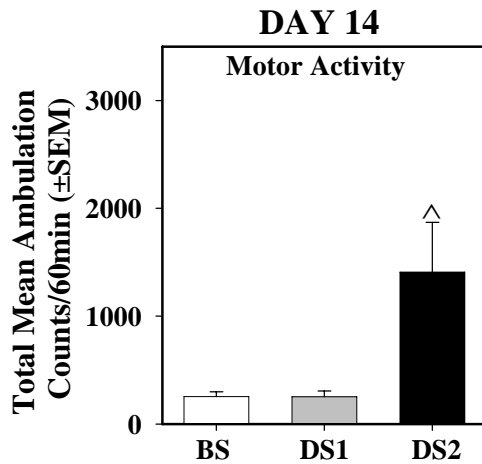


Figure 10. Intra-VTA Dermorphin-Saporin (Day 14 pretreatment) Increases Mean Total Ambulation

Effects of intra-VTA pretreatment with the μ -opioid receptor specific toxin dermorphin-saporin (DS) on mean total ambulation \pm SEM (60 min) for rats pretreated 14 days previously with B-S control (BS; n=11) or DS (DS1 or DS2; 1 or 2 pmol/200nl/side; n=11).

A two-way ANOVA indicated a main effect of pretreatment ($F_{2,22} = 6.78$, $p < 0.05$), a main effect of time ($F_{2,22} = 0.0054$, $p < 0.0001$, experiment 1), but not a significant treatment x time interaction, for mean total ambulation ($F_{2,22} = 1.08$, $p < 0.05$, **Figure 11**, experiment 1) on Day 14. Examination of the timecourse using individual one-way ANOVA and Fisher's LSD test indicated significant elevations of ambulatory motor activity for DS 2-treated rats relative to BS-treated rats ($p < 0.05$).

Effects of intra-VTA Microinjection of Dermorphin-Saporin on VTA mRNA Expression

Relative quantities of expression of GAD-67, μ -opioid receptor, and TH mRNA were assessed 7 or 14 days following pretreatment microinjection of BS or DS (1 or 2 pmol/200nl/side, experiment 1) into the VTA. The Wilcoxon Kruskal-Wallis test was used to determine significant differences with absolute p values. A main effect of pretreatment was observed. The $\Delta\Delta C_T$ (relative abundance) of GAD-67 and μ -opioid receptor mRNA was lower in the VTA from rats pretreated with either dose of DS compared to BS; these differences were not significant at day 7 for GAD-67 ($X^2 = 4.89$, $p > 0.05$) or μ -opioid receptor ($X^2 = 7.52$, $p < 0.05$, **Figure 12**). A significant difference between DS2-treated and BS-treated rats on day 14 for GAD-67 ($X^2 = 4.32$, $p < 0.05$) and for μ -opioid receptor mRNA ($X^2 = 5.84$, $p < 0.05$, **Figure 12**). The relative abundance of

TH mRNA was not different from rats pretreated with either dose of DS compared to BS; there were no differences evident at day 7 ($X^2 = 2.53$, $p > 0.05$) or day 14 ($X^2 = 2.53$, $p > 0.05$, **Figure 12**).

Figure 11.

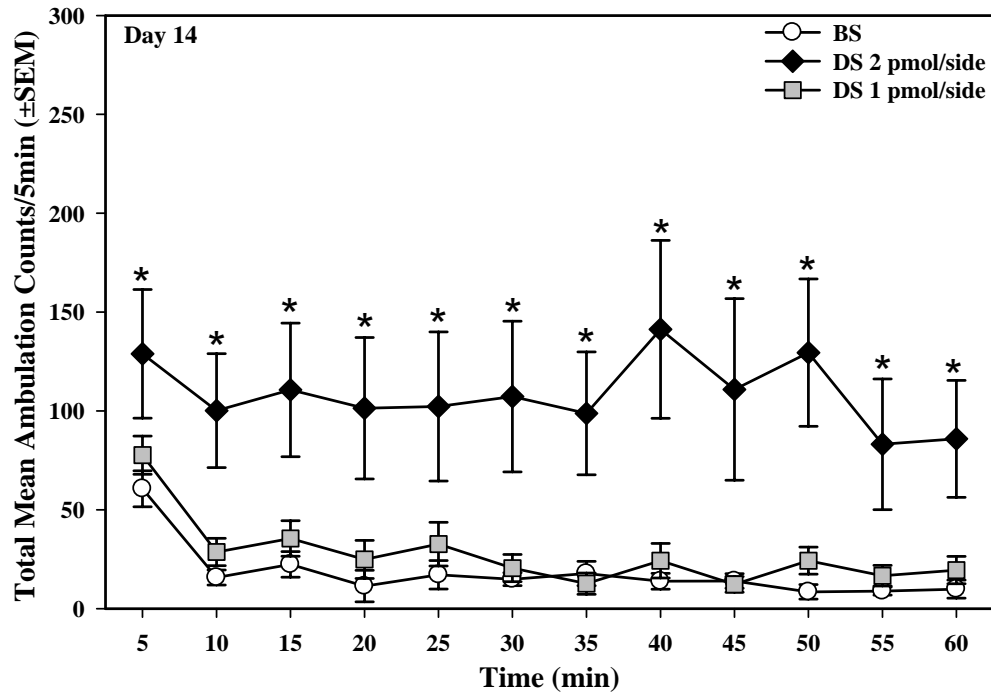


Figure 11. Elevated Ambulation at Day 14 after Intra-VTA Dermorphin-Saporin

Effects of intra-VTA pretreatment of the μ -opioid receptor specific toxin dermorphin-saporin (DS) on mean total ambulation in 5 min time bins (\pm SEM) for rats previously pretreated with BS control (BS; $n=11$) or DS (DS1 or DS2; 1 or 2 pmol/200nl/side; $n=11$) 14 days after pretreatment. * Ambulation levels that were significantly different from BS at the corresponding time point based upon Fisher's Least Significant Difference test.

Figure 12.

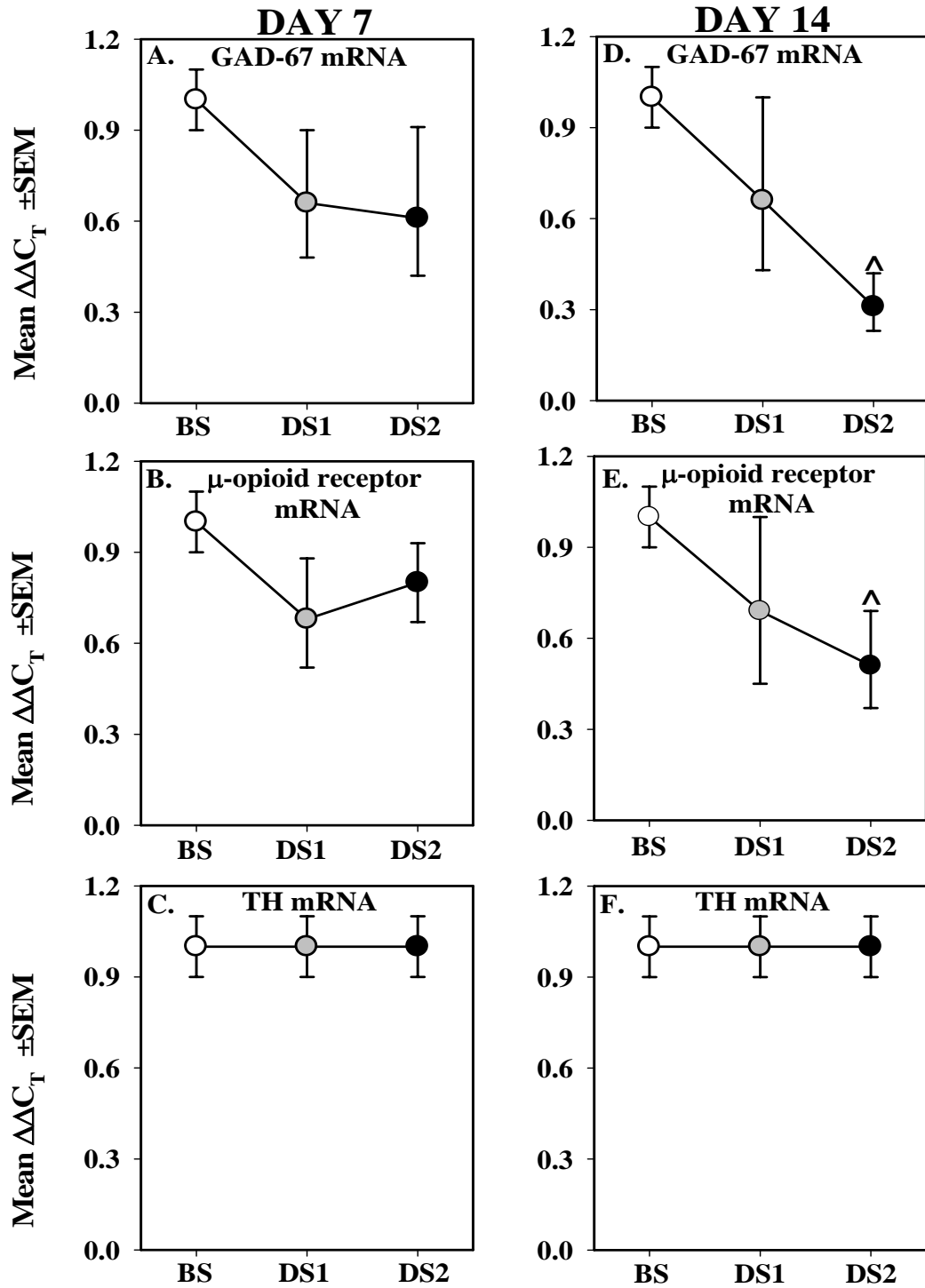


Figure 12. Intra-VTA Dermorphin-Saporin Lesions GABA-containing Neurons

Effects of intra-VTA administration of the μ -opioid receptor specific toxin dermorphin-saporin (DS) on mean $\Delta\Delta C_T$ (Mean \pm SEM) of three mRNA targets. Rats pretreated with BS control (BS; n=8) or D-S [1 (DS1) or 2 (DS2) pmol/200nl/side; n=8]. **Fig. 12A-C** Rats 7 days after pretreatment; **Fig. 12D-F** Rats 14 days after pretreatment. **A,D** Total activity. **B,E** Mean $\Delta\Delta C_T$ (relative abundance) of GAD-67 mRNA. **C,F** Mean $\Delta\Delta C_T$ (relative abundance) of μ -opioid receptor mRNA. The *asterisks* (*) indicates activity levels significantly different ($P<0.05$) from BS controls and DS1 pretreated animals, while the *caret* (^) indicates activity levels significantly different ($P<0.05$) from BS controls.

Effects of intra-VTA Microinjection of Dermorphin-Saporin on VTA Protein Expression

The ability of DS pretreatment to selectively ablate neurons in the VTA was visualized by immunohistochemical analyses for GAD-67 (black staining, **Figure 13**), μ -opioid receptors (black staining, **Figure 14**, experiment 1), TH protein (black staining, **Figure 15**) in the VTA. Cells and processes appear to be stained for GAD-67 in controls and the expression is not as evident after pretreatment with the highest dose of DS (DS2-treated) relative to BS-treated at day 7 and day 14 (**Figure 13**). Cells and processes appear to be stained for μ -opioid receptor in controls and the expression is not as evident after pretreatment with the highest dose of DS (DS2-treated) relative to BS-treated at day 7 and day 14 (**Figure 14**). This apparent decrease in GAD-67 and μ -opioid receptor was not evident at the lower dose of DS (DS1-treated) compared to BS-treated (**Figure 15**). Cells and processes appear to stain prominently for TH in controls and the expression is as evident in the DS-treated rats. Although there appeared to be reductions in the relative numbers of IR-positive cells, the images were not quantified due to local tissue damage effects that hampered immunostaining throughout a defined area but we were able to provide representative images of intact tissues obtained from treated animals.

Figure 13.

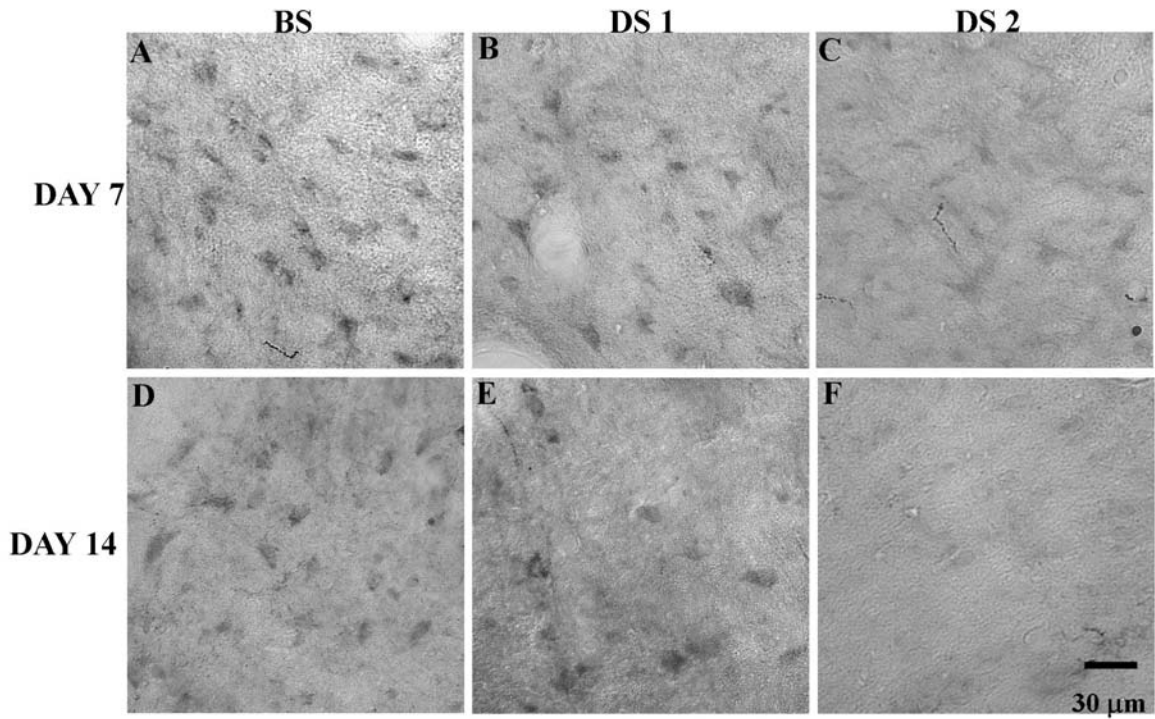


Figure 13. Intra-VTA Dermorphin-Saporin Appears to Decrease GAD-67-IR

Representative brightfield photomicrographs of GAD-67-IR (black staining) in coronal sections of the VTA (200x magnification, -6.0mm relative to bregma). Apparent decrease in the number of GAD-67-IR positive cells in the VTA after pretreatment (**Fig. 13B-C, 13E-F**). **A**, BS control (*BS*) **B**, DS 1 (*DS 1*; 1pmol/200nl/side) at day 7 recovery and **C**, DS (*DS 2*; 2pmol/200nl/side) at day 7 after pretreatment. **D**, BS control (*BS*), **E** DS (*DS 1*; 1pmol/200nl/side) and **F** DS (*DS 2*; 2pmol/200nl/side) at day 14 after pretreatment. The sample size was n=7 for all groups tested.

Figure 14.

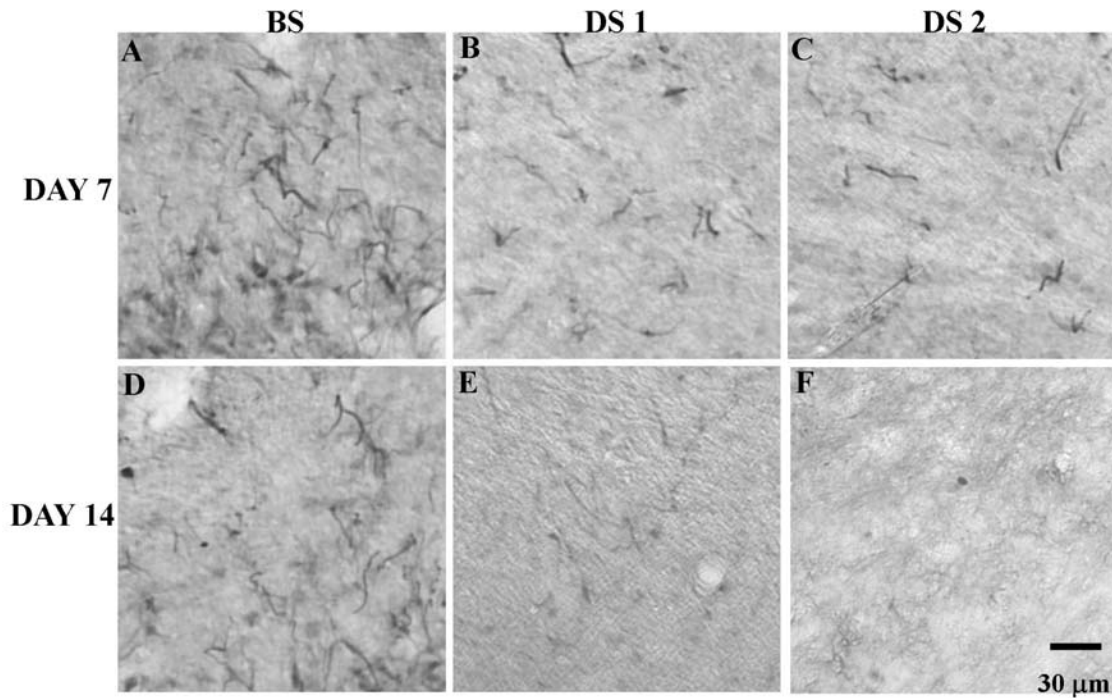


Figure 14. Intra-VTA Dermorphin-Saporin Appears to Decrease μ -Opioid Receptor-IR

Representative brightfield photomicrographs of μ -opioid-IR (black staining) in coronal sections of the VTA (200x magnification, -6.0mm relative to bregma). Apparent decrease in the number of μ -opioid-IR positive cells in the VTA after pretreatment (**Fig. 14B-C, 14E-F**). **A**, BS control (*BS*) **B**, DS (*DS1*; 1pmol/200nl/side) and **C**, DS (*DS2*; 2pmol/200nl/side) at day 7 after pretreatment. **D**, BS control (*BS*), **E** D-S (*DS1*; 1pmol/200nl/side) and **F** DS 2 (*DS2*; 2pmol/200nl/side) at day 14 after pretreatment. The sample size was n=7 for all groups tested.

Figure 15.

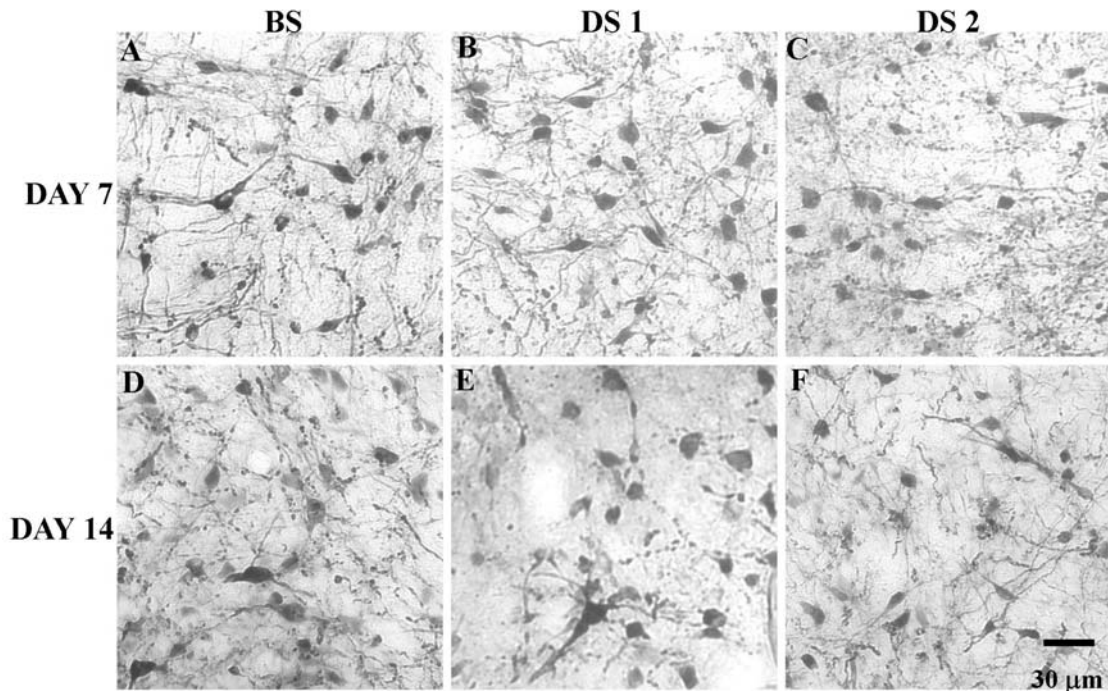


Figure 15. Intra-VTA Dermorphin-Saporin Appears to have no effect on Tyrosine Hydroxylase

Representative brightfield photomicrographs of TH-IR (black staining) in coronal sections of the VTA (200x magnification, -6.0mm relative to bregma). No change apparent in the number of TH-IR positive cells in the VTA is evident after pretreatment. **A**, BS control (*BS*) **B**, DS (*DS 1*; 1pmol/200nl/side) and **C**, D-S (*DS2*; 2pmol/200nl/side) at day 7 after pretreatment. **D**, BS control (*BS*), **E** D-S (*DS1*; 1pmol/200nl/side) and **F** D-S (*DS2*; 2pmol/200nl/side) at day 14 after pretreatment. The sample size was n=7 for all groups tested.

Effects of Intra-VTA Microinjection of Dermorphin-Saporin on Cocaine-evoked Hyperactivity

Mean total ambulation counts/60 min (\pm SEM) were assessed 7 days (**Figure 16**) following pretreatment with BS or DS (1.0 pmol/200nl/side, experiment 2) and treatment with saline (1 ml/kg, IP) or cocaine (10 mg/kg, IP). A two-way ANOVA indicated a main effect of pretreatment ($F_{1,23} = 28.46$; $p < 0.05$, **Figure 16**) as well as a main effect of treatment with cocaine ($F_{1,23} = 20.06$; $p < 0.05$, **Figure 16**), but no pretreatment x treatment interaction ($F_{1,23} = 0.43$; $p > 0.05$, **Figure 16**) on ambulation counts at day 7 after pretreatment.

Figure 16.

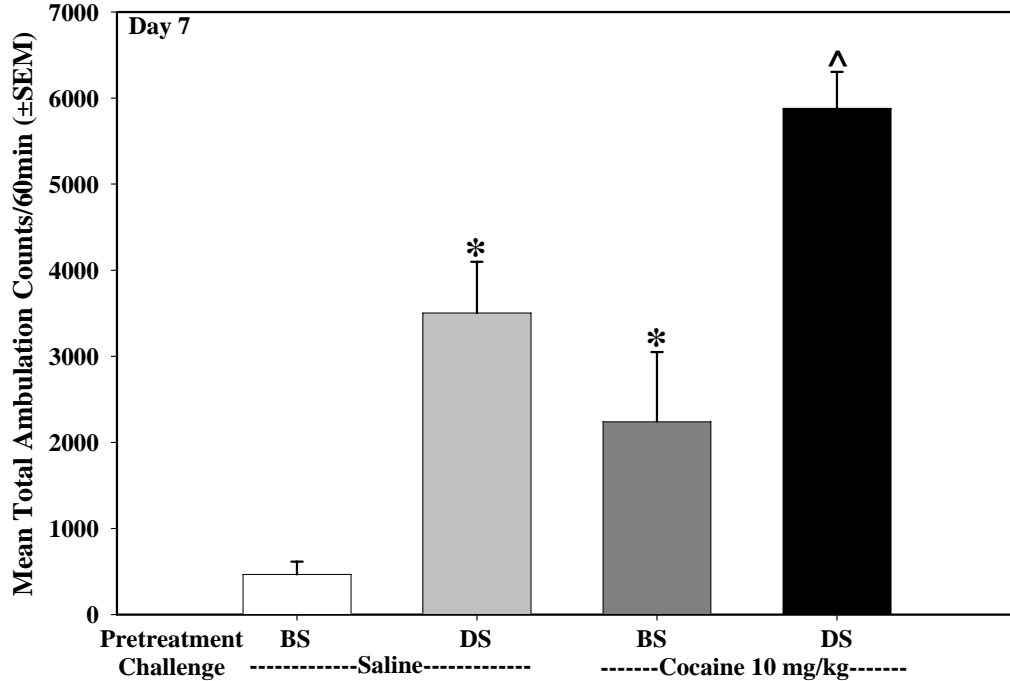


Figure 16. Elevated Baseline Activity with DS-pretreatment Predicts Elevated Cocaine-Induced Locomotor Activity

Effects of intra-VTA microinjection of dermorphin-saporin (DS) on cocaine-evoked hyperactivity in rats pretreated with BS control (BS; n=6) or DS (DSI, 1 pmol/200nl/side; n=6) followed by challenge treatment with saline (1ml/kg, IP) or cocaine (10 mg/kg, IP). Mean total ambulation (counts/60min; \pm SEM) in rats pretreated 7 days after pretreatment. The *asterisk* (*) indicates activity levels significantly different ($P<0.05$) from BS saline challenged controls, while the *caret* (^) indicates activity levels significantly different ($P<0.05$) from all other groups.

Utilizing a three-way ANOVA with time as a repeated measure, a main effect of pretreatment ($F_{1,20} = 33.59, p<0.05$, experiment 2), a main effect of treatment ($F_{1,20} = 18.54, p<0.05$), and no pretreatment x treatment x time interaction ($F_{1,11} = 1.83, p=0.05$) was shown for mean total ambulation (**Figure 17**). Examination of the timecourse using individual one-way ANOVA and Fisher's LSD test indicated significant differences across all time points relative to their individual controls (BS Saline).

Figure 17.

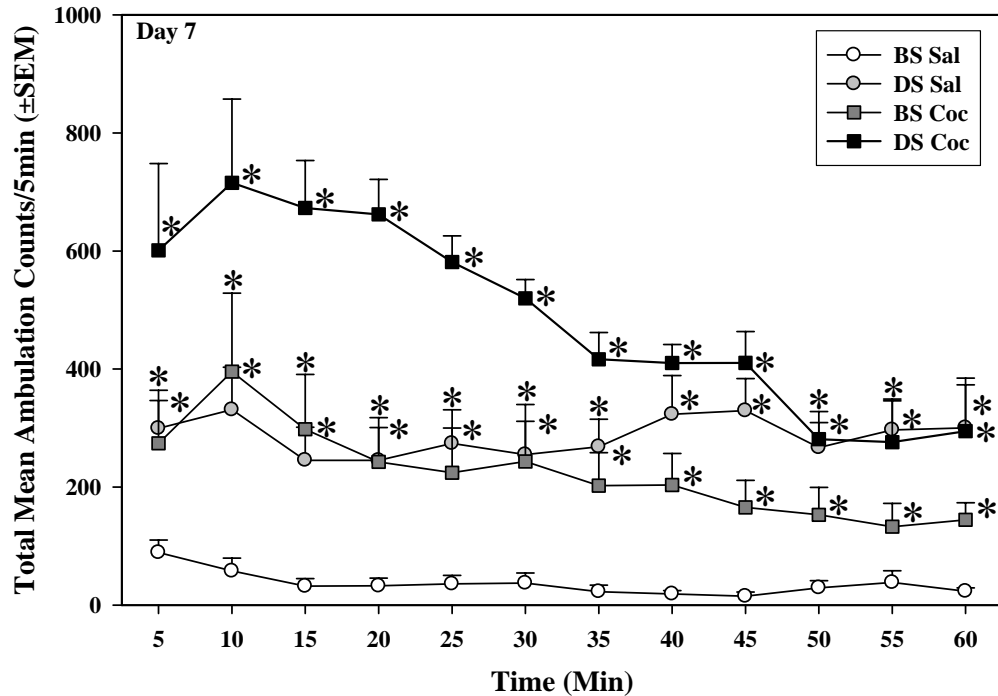


Figure 17. Combination of Intra-VTA Dermorphin-Saporin (Day 7 pretreatment) and Cocaine Challenge Increase Mean Total Ambulation across 60 min

Effects of intra-VTA microinjection of dermorphin-saporin (DS) on cocaine-evoked hyperactivity in rats pretreated with BS control (BS; n=6) or DS (DS1, 1 pmol/200nl/side; n=6) followed by challenge treatment with saline (1ml/kg, IP) or cocaine (10 mg/kg, IP). Timecourse of mean total ambulation plotted in 5 min bins across the 60 min test session following IP injection of saline or cocaine (10 mg/kg, IP). The *asterisk* (*) indicates activity levels significantly different ($P < 0.05$) from BS saline challenged controls

Mean total ambulation counts/60 min (\pm SEM) was assessed 14 days (**Figure 18**, experiment 2) following pretreatment with BS or DS (1.0 pmol/200nl/side) and treated with saline (1 ml/kg, IP) or cocaine (10 mg/kg, IP). A two-way ANOVA indicated that there was no main effect of pretreatment with DS ($F_{1,35} = 2.19$; $p > 0.05$, **Figure 18**), a main effect of treatment with cocaine ($F_{1,35} = 8.62$; $p < 0.05$, **Figure 18**), but no significant pretreatment x treatment interaction ($F_{1,35} = 3.52$; $p > 0.05$, **Figure 18**) on ambulation at day 14 days after pretreatment. The pretreatment x treatment interaction in the absence of a main effect of DS pretreatment indicates the pretreatment is essential to develop the magnitude of treatment (cocaine) response.

Figure 18.

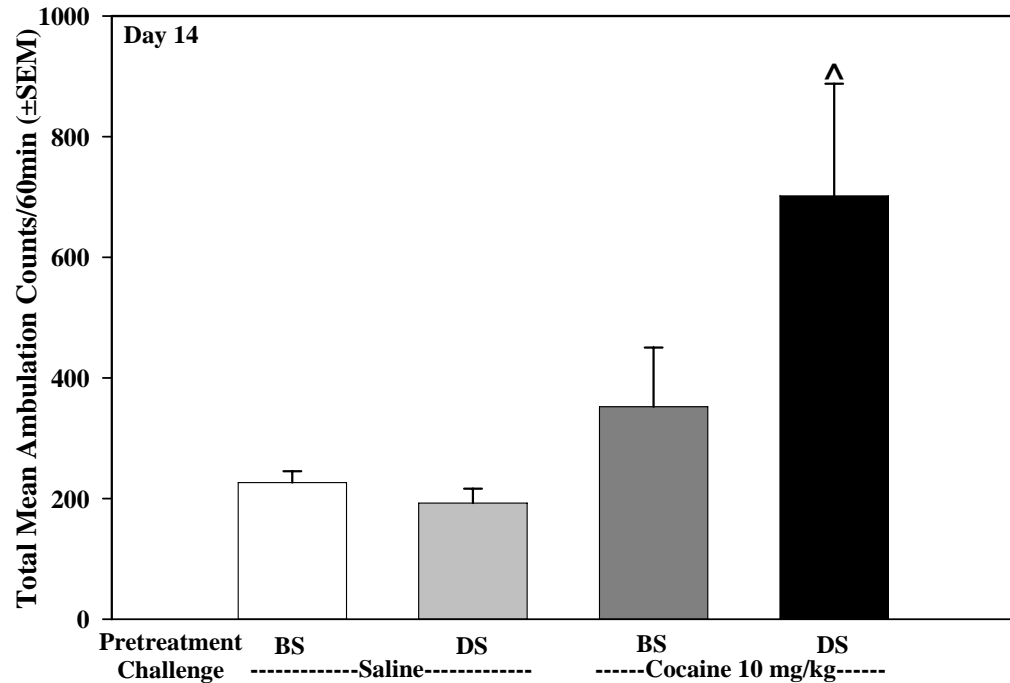


Figure 18. Combination of Intra-VTA Dermorphin-Saporin (Day 14 pretreatment) and Cocaine Challenge Increase Mean Total Ambulation

Effects of intra-VTA microinjection of dermorphin-saporin (D-S) on cocaine-evoked hyperactivity in rats pretreated with BS control (BS; n=9) or DS (DSI, 1 pmol/200nl/side; n=9) followed by challenge treatment with saline (1ml/kg, IP) or cocaine (10 mg/kg, IP). Mean total ambulation (counts/60min; \pm SEM) in rats pretreated 14 days after pretreatment. The *asterisk* (*) indicates activity levels significantly different ($P < 0.05$) from BS saline challenged controls, while the *caret* (^) indicates activity levels significantly different ($P < 0.05$) from all other groups.

Figure 19.

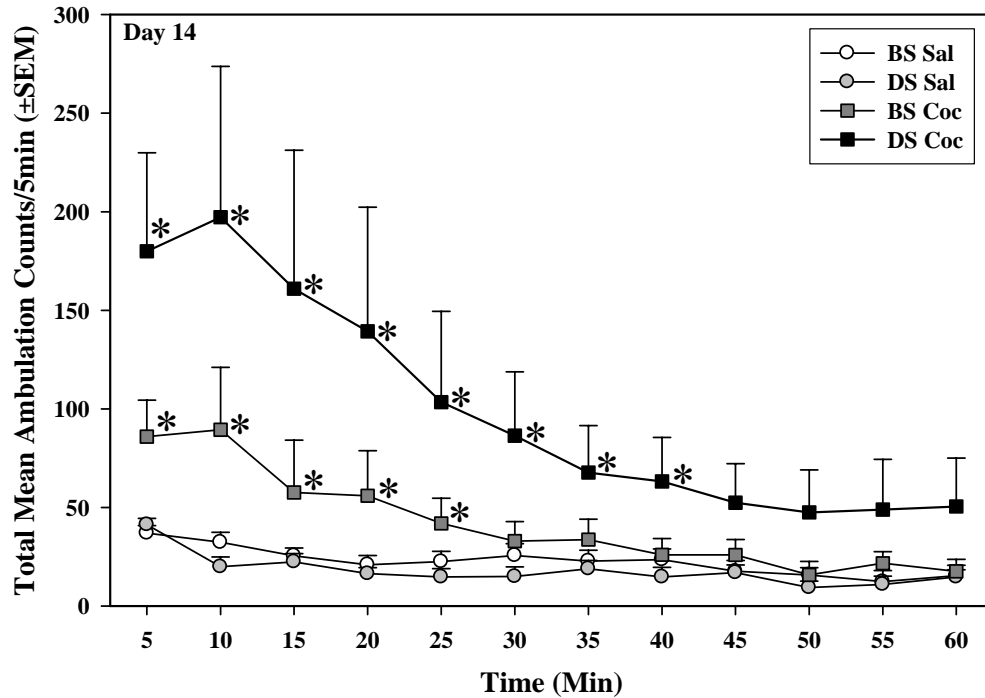


Figure 19. Combination of Intra-VTA Dermorphin-Saporin (Day 14 pretreatment) and Cocaine Challenge Increase Mean Total Ambulation across 60 min

Effects of intra-VTA microinjection of dermorphin-saporin (DS) on cocaine-evoked hyperactivity in rats pretreated with BS control (BS; $n=9$) or DS (DS1, 1 pmol/200nl/side; $n=9$) followed by challenge treatment with saline (1ml/kg, IP) or cocaine (10 mg/kg, IP). Timecourse of mean total ambulation plotted in 5 min bins across the 60 min test session following IP injection of saline or cocaine (10 mg/kg, IP). The asterisk (*) indicates activity levels significantly different ($P < 0.05$) from BS saline challenged controls.

Utilizing a three-way ANOVA with time as a repeated measure, no main effect of pretreatment ($F_{1,20} = 1.87$, $p > 0.05$, experiment 2), a main effect of treatment ($F_{1,20} = 9.18$, $p < 0.05$), and no significant pretreatment x treatment x time interaction ($F_{1,11} = 1.04$, $p > 0.05$) was shown for mean total ambulation (Figure 19), separated into 12 different 5-min time bins when comparing both DS1 and DS2 to BS saline controls. Examination of the timecourse using individual one-way ANOVA and Fisher's LSD test indicated a significant differences across some of the points relative to controls (BS Saline; * $p < 0.05$).

DISCUSSION

The aim of this study was to examine the role of VTA GABA-containing neurons in the modulation of basal locomotor activity and cocaine-evoked hyperactivity. The VTA is predominately populated by two types of neurons, DA-containing and GABA-containing neurons (Johnson and North, 1992b); μ -opioid receptors in the VTA are localized primarily on the GABAergic cells (Garzon and Pickel, 2001). Thus the conjugated toxin DS was utilized to specifically ablate GABA-containing neurons within the VTA. We have shown here that destruction of GABAergic neurons in the VTA resulted in a dose-dependent increase in basal motor activity most evident at the earliest timepoint of analysis (day 7) after treatment. Animals pretreated with the toxin exhibited significant loss of mRNA for GAD-67 and μ -opioid receptors, but not for TH, as indicated by mRNA markers. The loss of mRNA for GAD-67 and μ -opioid receptors was mirrored by an apparent loss in protein expression for these 2 markers. Therefore, we confirmed a selective ablation of GABA-containing neurons without evidence of significant damage to DA neurons.

The magnitude of changes in spontaneous motor activity following a single infusion of toxin into the VTA was dependent upon the toxin dose and the time period after which behavioral and levels of molecular analyses were conducted. Basal motor activity on day 7 was significantly elevated after either dose of the toxin, and molecular markers (GAD-67 and μ -opioid receptor mRNA) showed a non-significant decrease (**Figure 12**). The later timepoint of analysis (day 14) represents a snapshot of normalizing basal activity in the face of accelerating losses in molecular markers for GABA-containing neurons, noted to be significant after the high dose of toxin pretreatment. Thus, the behavioral consequences of the toxin occur predominantly during the period in which GABA-containing neurons appear to be degrading and dying. At the point at which we observe the only significant molecular changes (day 14), basal activity has completely (low dose) or partially (high dose) normalized to control levels, although control levels for day 14 are different than those from day 7.

These data suggest that compensatory mechanisms may be responsible for the normalizing basal activity in the face of the toxin lesion of the VTA. The dose-dependent increases in locomotor activity at the earliest timepoint (day 7) are likely due to dose-dependent damage or loss of local GABA-containing neurons, which would be expected

to result in a disinhibition of DA-containing cell firing and increased motor activity (Di Chiara and Imperato, 1988b; O'Brien and White, 1987). The mechanisms underlying the normalization of basal activity of DS1-treated animals and the near-normalization of DS2-treated animals at day 14 after infusion are likely based on compensatory responses in this system were not directly explored in the present set of experiments. It is possible, for example that return to baseline levels of spontaneous activity is related to an increase of GABA release (Bonci and Williams, 1997) from the remaining local GABA-containing neurons or an increase in GABA release from other afferents. Additionally, GABA receptors located on VTA DA-containing neurons could potentially be up-regulated (Barnes, Jr., 1996) and thus confer a greater sensitivity to the limited GABA neurotransmitter availability. Furthermore, a change in the basal state of local DA-containing neurons could also be responsible for a return to behavioral baseline, either intrinsically by decreases in NAc DA (Taber et al., 1996) release or a downregulation of the DA postsynaptic receptor systems (Hall et al., 1998), potentially in the NAc. Lastly, other neurotransmitter systems in the VTA could contribute to the normalization of spontaneous motor activity and those that normally tonically inhibit VTA DA neurons and decrease NAc DA release are particularly suspect because they may function in a similar manner as the GABA-containing neurons that were lesioned in the VTA.

Compensative mechanisms may result in an overt normalization of spontaneous motor activity by day 14 after infusion of DS, however, administration of cocaine reveals that ablation of GABA-containing neurons still has important behavioral consequences. Thus, in the face of normalizing basal activity after the toxin lesion of the VTA, the ability of cocaine to evoke hyperactivity remains intact, suggesting that the compensatory mechanisms responsible for the normalization of locomotor activity have no direct effect on the ability to generate cocaine-evoked hyperactivity and that VTA function is still unbalanced and not completely normalized. This is surprising because locomotor activity induced by cocaine are mediated in large part via the mesoaccumbens pathway (Kalivas and Nakamura, 1999). Thus, the GABA inhibition of VTA DA-containing neurons may not modulate motor hyperactivity induced by cocaine administration.

The selectivity and extent of DS pretreatment was assessed utilizing quantitative real-time PCR for transcripts specific for GAD-67, μ -opioid receptors and TH. Utilizing mRNA allowed us to dissect the VTA of lesioned animals and to quantify molecular

markers specifically for GABA-containing and DA-containing neurons in the VTA. The quantification of specific mRNA targets in the VTA allowed us to determine which neuronal populations were impacted by DS infusion. The reduction of mRNA for GAD-67 and μ -opioid receptors indicates a selective loss of GABA-containing neurons in the VTA after DS pretreatment even after the locomotor activity has returned to baseline, which suggests that the neurons that generate these markers are not regenerated by day 14. The lack of effect on TH indicated no effect on VTA DA neurons indicates that DA mRNA levels remain stable even after VTA GABA neurons are lesioned.

The selectivity of DS for GABA-containing neurons was further assessed by visualization of VTA tissue after toxin pretreatment and immunolabeling for antibodies corresponding to the protein targets of GAD-67, μ -opioid receptors, and TH. Quantification of cell numbers in our tissue samples was not possible because each of the antibodies displayed a unique staining profile and the injection/lesioning process itself caused tissue damage which hampered the ability to conclusively count cells in a defined area. The visualization of representative immunostaining allows us to speculate as to the impact of toxin pretreatment. The DS pretreatment appeared to cause no effect at day 7 after pretreatment and a potential relative reduction in μ -opioid receptor and GAD-67 immunoreactivity after 2 weeks, with no relative difference in TH. Defining the extent of toxin damage utilizing immunolabels may not be the best approach for quantification for a variety of reasons, including the possibility of positive immunolabeling on non-functional cells as indicated by infiltration of microglia to the injection sites between days 4 and 7 (Seeger et al., 1997) which may hold molecular targets in place until the microglia clear the detritus. Thus we chose to utilize the mRNA to quantify the extent of toxin damage as well as visualization of immunolabeled tissue to gain further insight into molecular changes after toxin pretreatment.

The loss of GABA-containing neurons in the VTA results in increased locomotor activity, presumably via disinhibition of DA-containing neurons and downstream increases in NAc DA efflux, which is well-known to be correlated with increases in locomotor activity in drugs abused by humans (Di Chiara and Imperato, 1988b). This mechanism is supported by numerous pharmacological studies involving GABA mimetics. For example, local blockade of GABA receptors by selective antagonists mirrors our results of GABA-containing neuron ablation, by temporarily interrupting

tonically inhibitory GABA neurons. In particular, intra-VTA blockade of postsynaptic GABA_A receptors with either picrotoxin or bicuculline increases DA efflux in the NAc which is attenuated with co-administration of the GABA_A agonist muscimol (Ikemoto et al., 1997a) and this is further supported by the demonstration that picrotoxin is readily self-administered into the VTA (Ikemoto et al., 1997b). Furthermore, intra-VTA administration of the GABA_B agonist baclofen blocked morphine induced hyperactivity (Leite-Morris et al., 2002), indicating that VTA GABA receptors are important in drug-induced locomotion. Thus, not only do GABA-containing neurons of the VTA modulate basal locomotor activity, but they are also important in the modulation of locomotor behaviors generated by drugs of abuse.

The population of μ -opioid expressing GABA-containing neurons in the VTA are critically involved in the expression of both basal as well as cocaine-evoked locomotor activity. Additionally, the ability of animals to normalize to basal levels two weeks after selective VTA GABA-containing neuron ablation, indicates a prominent and robust modulation of VTA DA-containing neurons. These data provide valuable insights into regulation of basal- and drug-induced locomotion and also provide a new strategy to further test the ability of VTA DA-containing neurons to react to substantial changes in local circuitry.

CHAPTER 4

Overall Conclusions

INTRODUCTION

A thorough understanding of the VTA CB₁R and modulation of GABA inhibition of VTA DA-containing neurons is of paramount importance in drug abuse research. We have provided a detailed description of the heterogeneity of VTA CB₁R populations, evidence for postsynaptic CB₁R expression within cells of the VTA, as well as a potential subnucleus within the VTA that may be critical in terms of drug reward and reinforcement neurotransmission. Furthermore, we have provided evidence that demonstrates the importance of VTA GABA neurons in basal as well as psychostimulant-induced locomotor activity and these data have provided a novel strategy to study the regulatory mechanisms of VTA DA-containing neurons and their normalization after changes in VTA neuronal populations.

The overall topography of innervation of the VTA is considered a complex “linked network” (Geisler and Zahm, 2005) amongst many different brain nuclei. The complexity of the VTA extends beyond specific cells within the VTA to systems interconnected with the VTA. For example, while the VTA contains cell bodies of DA-containing and GABA-containing neurons (Johnson and North, 1992b; Mathon et al., 2003), in addition the VTA receives innervation from numerous other neurotransmitter systems, such as glutamate, acetylcholine, serotonin, noradrenaline, enkephalin as well as many others (Mathon et al., 2003) including the endogenous cannabinoid neurotransmitter system (present study; Melis et al., 2004; Schlicker and Kathmann, 2001; Szabo et al., 2002; Wenger et al., 2003). A subset of the VTA DA-containing neurons project to limbic areas such as the NAc and comprise the mesoaccumbens pathway (Swanson, 1982c), while GABA-containing neurons in the VTA serve as both local interneurons as well as projection neurons (Carr and Sesack, 2000; Nagai et al., 1983; Steffensen et al., 1998; Van Bockstaele and Pickel, 1995). The combination of the resident neuronal populations, interconnected circuits, and the diverse neurotransmitter systems which all impact the VTA suggests a potentially high degree of heterogeneity or region-specific receptor expression of CB₁R within the VTA.

The heterogeneity of the VTA extends beyond resident neuronal populations but also to receptor localization, which may impact functional output such as behavior. We have demonstrated a rostrocaudal gradient of CB₁R localization in the IF VTA subnucleus as well as heterogeneity throughout the entire VTA. Cannabinoid-evoked protein expression and behavior evoked after cannabinoid administration have also been shown to be heterogenous within the VTA. This heterogeneity is evident in recent reports that demonstrate systemically-administered cannabinoids can differentially alter the expression levels of protein expression across VTA subnuclei. Thus, taken together, these data as well as our demonstration of high levels of CB₁R in the caudal IF as well as the heterogenous CB₁R VTA protein expression suggest that regional differences in the actions and potential expression of CB₁R in the VTA may differentially modulate locomotor effects and protein expression after cannabinoid administration.

The regiospecificity of CB₁R localization in the VTA is further complicated by the synaptic localization of these receptors. The CB₁R has been functionally localized to presynaptic terminals of both GABA (Szabo et al., 2002) and glutamate terminals (Melis et al., 2004) in the VTA, suggesting that CB₁R modulates inhibitory as well as excitatory input to VTA neurons. Currently, CB₁R are thought to be localized primarily presynaptically, although there are numerous reports of postsynaptic CB₁R localization (Endoh, 2006; Hohmann et al., 1999; Kelly and Chapman, 2001; Kirby et al., 2000; Lopez-Redondo et al., 1997; Pickel et al., 2004; Rodriguez et al., 2001; Salio et al., 2002; Schweitzer, 2000) and now we demonstrated evidence of postsynaptic localization of CB₁R in the VTA. The ample evidence of postsynaptic CB₁R populations throughout various brain areas supports our data as we are first to describe CB₁R-IR located on cell bodies within the VTA and provide an important advance in understanding how cannabinoids modulate neurotransmission in the mesocorticolimbic circuits. The development of detailed localization of pre- and postsynaptic VTA CB₁R populations and their potential functional overlap may hold the key to understanding VTA CB₁R modulation of locomotor activity and ultimately marijuana abuse.

The possibility of a solitary mechanism of action for CB₁R in the VTA that accounts for drug reward mechanisms is unlikely. Our understanding of the components of endogenous cannabinoid signaling in the VTA is important to gain clues as to the function of this receptor in drug abuse. One current hypothesis is that endocannabinoid

release is suggested to be part of an “on-demand” compensatory response to promote repair and cell survival in response to a variety of signals (Karanian and Bahr, 2006). While potentially located both pre- and postsynaptically in the VTA, the CB₁R is poised to regulate both afferents and efferents of the VTA. Thus our demonstration of a previous undefined population of CB₁R in the VTA could be indicative of receptors expressed at critical locations required for this putative compensatory response system. Understanding the impact of drug abuse on reward circuit signaling is clearly important and developing a better understanding of how these circuits compensate for modulated neurotransmission “under the influence” of drugs of abuse will ultimately lead to better pharmacotherapies to counteract addiction.

Several animal models of reward/reinforcement have demonstrated the role of GABA neurotransmission in the VTA in regulating the reinforcing and rewarding effects of various drugs of abuse (Corrigall et al., 1999; Corrigall et al., 2000; David et al., 1997; Xi and Stein, 1999). A variety of receptors including the CB₁R (Szabo et al., 2002) and μ -opioid receptors (Johnson and North, 1992a) have been implicated in the modulation of GABA neurotransmission in the VTA. The hyperpolarization of VTA GABA-containing neurons results in a disinhibition of the principal DA-containing neurons (Johnson and North, 1992a) and may cause a switch to burst firing and increased firing frequency of these DA-containing neurons (Miller et al., 1981; Overton and Clark, 1997). This leads to a downstream efflux of DA in the NAc and subsequent increases in locomotor activity, effects that are common with administration of drugs of abuse (Di Chiara and Imperato, 1988b). Thus our demonstration that selective ablation of GABA-containing neurons in the VTA increased spontaneous locomotor activity and potentiated cocaine-induced hyperactivity, suggests that GABA-containing neurons in the VTA play an important inhibitory role on the activation of basal and drug-induced locomotor activity.

Our studies of GABA-containing neuronal ablation in the VTA have yielded more than just the observation that we increased locomotor activity by removing a subset of the local GABA neurons. The repeated observation of the return to basal activity levels 14 days after pretreatment indicates prominent and robust compensatory systems that have yet to be explored. Our studies provide the basis for developing a novel strategy for understanding what drives DA modulation and behavior back to basal levels after decreasing GABA input. These studies provide a springboard into understanding the

reaction of a set of neurocircuits in response to insult and injury and may ultimately provide evidence as to how these circuits respond to drugs of abuse.

The functional consequences of removing a portion of the inhibitory control of VTA DA-containing neurons not only may yield important insights into drug use but also into other phenomenon that impact drug use. For example, DA impulse activity has been implicated in learning and memory (Cooper, 2002; Grace, 2000), as well as been associated with individual vulnerability to the reinforcing effects of cocaine and other drugs of abuse (Marinelli et al., 2003). In addition, decreased DA impulse activity is associated with reduced vulnerability to self-administer cocaine, while increased activity is an indicator of an increased propensity to self-administer cocaine (Marinelli and White, 2000; Marinelli et al., 2003). Thus, the potential exists that an imbalance in the modulation of DA impulse activity by decreased levels GABA inhibition could be an indicator of a greater propensity to self-administer drugs of abuse such as cocaine. Clearly, developing a better understanding of the impact GABA neuron removal on DA impulse activity is an important compensatory mechanism that needs to be developed further.

OVERALL SUMMARY

In conclusion, the present studies demonstrated a heterogenous CB₁R population in the VTA as well as a gradient of increasing CB₁R localization (from rostral to caudal) in the IF of the VTA and further evidence of postsynaptic CB₁Rs. The areas of highest CB₁R expression correspond spatially to the coordinates at which local GABA-containing neurons were found to be modulators of basal and cocaine-evoked hyperactivity. These studies provide evidence that the caudal VTA is an important nucleus of CB₁R expression as well as GABA modulation of basal and cocaine-evoked activity. This discrete caudal nucleus of the VTA may be critical in the development of pharmacological tools for treatment and intervention strategies of drug abuse. The similarity of the neural circuitry underlying reward in humans and drug-induced hyperactivity in rodents suggests that caudal VTA CB₁R should be further investigated as a potential site for pharmacological intervention in drug abuse.

Most importantly, these studies have laid the foundation for understanding compensatory mechanisms in the VTA. First, by expounding upon the hypothesis that

VTA CB₁R may be part of an intrinsic compensatory mechanism that promotes repair and cell survival after insult/injury and the development of more accurate localization studies including this one are critical to advance our understanding of which neurons are affected by this mechanism. Secondly, the demonstration of the behavioral consequences of GABA ablation in the VTA and the subsequent return to baseline via some type of compensatory mechanism or mechanisms as well. Ultimately, these studies have started an understanding of the activation of compensatory mechanisms and further research after drug administration will yield critical knowledge in our desire to eradicate drug abuse and addiction.

Reference List

- Akema T, He D, Sugiyama H (2005) Lipopolysaccharide increases gamma-aminobutyric acid synthesis in medial preoptic neurones in association with inhibition of steroid-induced luteinising hormone surge in female rats. *J Neuroendocrinol* 17:672-678.
- Ameri A (1999) The effects of cannabinoids on the brain. *Prog Neurobiol* 58:315-348.
- Ashton JC, Appleton I, Darlington CL, Smith PF (2004a) Cannabinoid CB1 receptor protein expression in the rat choroid plexus: a possible involvement of cannabinoids in the regulation of cerebrospinal fluid. *Neurosci Lett* 364:40-42.
- Ashton JC, Appleton I, Darlington CL, Smith PF (2004b) Immunohistochemical localization of cannabinoid CB1 receptor in inhibitory interneurons in the cerebellum. *Cerebellum* 3:222-226.
- Ashton JC, Appleton I, Darlington CL, Smith PF (2004c) Immunohistochemical localization of cerebrovascular cannabinoid CB1 receptor protein. *J Cardiovasc Pharmacol* 44:517-519.
- Ashton JC, Darlington CL, Smith PF (2006a) Co-distribution of the cannabinoid CB1 receptor and the 5-HT transporter in the rat amygdala. *Eur J Pharmacol* 537:70-71.
- Ashton JC, Friberg D, Darlington CL, Smith PF (2006b) Expression of the cannabinoid CB2 receptor in the rat cerebellum: an immunohistochemical study. *Neurosci Lett* 396:113-116.
- Ashton JC, Zheng Y, Liu P, Darlington CL, Smith PF (2004d) Immunohistochemical characterisation and localisation of cannabinoid CB1 receptor protein in the rat vestibular nucleus complex and the effects of unilateral vestibular deafferentation. *Brain Res* 1021:264-271.
- Barnes EM, Jr. (1996) Use-dependent regulation of GABAA receptors. *Int Rev Neurobiol* 39:53-76.
- Bergevin A, Girardot D, Bourque MJ, Trudeau LE (2002) Presynaptic mu-opioid receptors regulate a late step of the secretory process in rat ventral tegmental area GABAergic neurons. *Neuropharmacology* 42:1065-1078.
- Bonci A, Williams JT (1997) Increased probability of GABA release during withdrawal from morphine. *J Neurosci* 17:796-803.
- Bowery NG, Hudson AL, Price GW (1987) GABAA and GABAB receptor site distribution in the rat central nervous system. *Neuroscience* 20:365-383.
- Bubar MJ, Pack KM, Frankel PS, Cunningham KA (2004) Effects of dopamine D1- or D2-like receptor antagonists on the hypermotive and discriminative stimulus effects of (+)-MDMA. *Psychopharmacology (Berl)* 173:326-336.

Burgess SE, Gardell LR, Ossipov MH, Malan TP, Jr., Vanderah TW, Lai J, Porreca F (2002) Time-dependent descending facilitation from the rostral ventromedial medulla maintains, but does not initiate, neuropathic pain. *J Neurosci* 22:5129-5136.

Butovsky E, Juknat A, Goncharov I, Elbaz J, Eilam R, Zangen A, Vogel Z (2005) In vivo up-regulation of brain-derived neurotrophic factor in specific brain areas by chronic exposure to Delta-tetrahydrocannabinol. *J Neurochem* 93:802-811.

Carr DB, Sesack SR (2000) GABA-containing neurons in the rat ventral tegmental area project to the prefrontal cortex. *Synapse* 38:114-123.

Cheer JF, Wassum KM, Heien ML, Phillips PE, Wightman RM (2004) Cannabinoids enhance subsecond dopamine release in the nucleus accumbens of awake rats. *J Neurosci* 24:4393-4400.

Chen J, Paredes W, Lowinson JH, Gardner EL (1990) Delta 9-tetrahydrocannabinol enhances presynaptic dopamine efflux in medial prefrontal cortex. *Eur J Pharmacol* 190:259-262.

Chen SR, Pan HL (2006) Loss of TRPV1-expressing sensory neurons reduces spinal mu opioid receptors but paradoxically potentiates opioid analgesia. *J Neurophysiol* 95:3086-3096.

Cooper DC (2002) The significance of action potential bursting in the brain reward circuit. *Neurochem Int* 41:333-340.

Corrigall WA, Coen KM, Adamson KL, Chow BL (1999) The mu opioid agonist DAMGO alters the intravenous self-administration of cocaine in rats: mechanisms in the ventral tegmental area. *Psychopharmacology (Berl)* 141:428-435.

Corrigall WA, Coen KM, Adamson KL, Chow BL, Zhang J (2000) Response of nicotine self-administration in the rat to manipulations of mu-opioid and gamma-aminobutyric acid receptors in the ventral tegmental area. *Psychopharmacology (Berl)* 149:107-114.

Creese I, Iversen SD (1973) Blockage of amphetamine induced motor stimulation and stereotypy in the adult rat following neonatal treatment with 6-hydroxydopamine. *Brain Res* 55:369-382.

Dahlstrom A, Fuxe K (1964) Localization of monoamines in the lower brain stem. *Experientia* 20:398-399.

David V, Durkin TP, Cazala P (1997) Self-administration of the GABAA antagonist bicuculline into the ventral tegmental area in mice: dependence on D2 dopaminergic mechanisms. *Psychopharmacology (Berl)* 130:85-90.

De Vries TJ, Shippenberg TS (2002) Neural systems underlying opiate addiction. *J Neurosci* 22:3321-3325.

- Devane WA, Dysarz FA, III, Johnson MR, Melvin LS, Howlett AC (1988) Determination and characterization of a cannabinoid receptor in rat brain. *Mol Pharmacol* 34:605-613.
- Di Chiara G, Imperato A (1988a) Opposite effects of mu and kappa opiate agonists on dopamine release in the nucleus accumbens and in the dorsal caudate of freely moving rats. *J Pharmacol Exp Ther* 244:1067-1080.
- Di Chiara G, Imperato A (1988b) Drugs abused by humans preferentially increase synaptic dopamine concentrations in the mesolimbic system of freely moving rats. *Proc Natl Acad Sci U S A* 85:5274-5278.
- Endoh T (2006) Pharmacological characterization of inhibitory effects of postsynaptic opioid and cannabinoid receptors on calcium currents in neonatal rat nucleus tractus solitarius. *Br J Pharmacol* 147:391-401.
- Erinoff L, Brown RM (1994) Neurobiological models for evaluating mechanisms underlying cocaine addiction. Washington, DC.: US Government Printing Office.
- Falk T, Zhang S, Erbe EL, Sherman SJ (2006) Neurochemical and electrophysiological characteristics of rat striatal neurons in primary culture. *J Comp Neurol* 494:275-289.
- Felder CC, Veluz JS, Williams HL, Briley EM, Matsuda LA (1992) Cannabinoid agonists stimulate both receptor- and non-receptor-mediated signal transduction pathways in cells transfected with and expressing cannabinoid receptor clones. *Mol Pharmacol* 42:838-845.
- Frankel PS, Cunningham KA (2002) The hallucinogen d-lysergic acid diethylamide (d-LSD) induces the immediate-early gene c-Fos in rat forebrain. *Brain Res* 958:251-260.
- French ED (1997) delta9-Tetrahydrocannabinol excites rat VTA dopamine neurons through activation of cannabinoid CB1 but not opioid receptors. *Neurosci Lett* 226:159-162.
- French ED, Dillon K, Wu X (1997) Cannabinoids excite dopamine neurons in the ventral tegmentum and substantia nigra. *Neuroreport* 8:649-652.
- Fu WJ, Hu J, Spencer T, Carroll R, Wu G (2006) Statistical models in assessing fold change of gene expression in real-time RT-PCR experiments. *Comput Biol Chem* 30:21-26.
- Gardner EL (2002) Addictive potential of cannabinoids: the underlying neurobiology. *Chem Phys Lipids* 121:267-290.
- Gardner EL (2005) Endocannabinoid signaling system and brain reward: emphasis on dopamine. *Pharmacol Biochem Behav* 81:263-284.
- Gardner EL, Vorel SR (1998) Cannabinoid transmission and reward-related events. *Neurobiol Dis* 5:502-533.

- Garzon M, Pickel VM (2002) Ultrastructural localization of enkephalin and mu-opioid receptors in the rat ventral tegmental area. *Neuroscience* 114:461-474.
- Garzon M, Pickel VM (2001) Plasmalemmal mu-opioid receptor distribution mainly in nondopaminergic neurons in the rat ventral tegmental area. *Synapse* 41:311-328.
- Geisler S, Zahm DS (2005) Afferents of the ventral tegmental area in the rat-anatomical substratum for integrative functions. *J Comp Neurol* 490:270-294.
- German DC, Manaye KF (1993a) Midbrain dopaminergic neurons (nuclei A8, A9, and A10): three-dimensional reconstruction in the rat. *J Comp Neurol* 331:297-309.
- Gessa GL, Melis M, Muntoni AL, Diana M (1998) Cannabinoids activate mesolimbic dopamine neurons by an action on cannabinoid CB1 receptors. *Eur J Pharmacol* 341:39-44.
- Gonzalez S, Mena MA, Lastres-Becker I, Serrano A, de Yebenes JG, Ramos JA, Fernandez-Ruiz J (2005) Cannabinoid CB(1) receptors in the basal ganglia and motor response to activation or blockade of these receptors in parkin-null mice. *Brain Res* 1046:195-206.
- Grace AA (2000) The tonic/phasic model of dopamine system regulation and its implications for understanding alcohol and psychostimulant craving. *Addiction* 95 Suppl 2:S119-S128.
- Greenamyre JT, Young AB, Penney JB (1984) Quantitative autoradiographic distribution of L-[3H]glutamate-binding sites in rat central nervous system. *J Neurosci* 4:2133-2144.
- Grubb MC, Welch JR, Finn DA, Mark GP (2002) Cocaine self-administration alters the locomotor response to microinjection of bicuculline into the ventral tegmental area of rats. *Brain Res* 952:44-51.
- Gysling K, Wang RY (1983) Morphine-induced activation of A10 dopamine neurons in the rat. *Brain Res* 277:119-127.
- Hall FS, Wilkinson LS, Humby T, Inglis W, Kendall DA, Marsden CA, Robbins TW (1998) Isolation rearing in rats: pre- and postsynaptic changes in striatal dopaminergic systems. *Pharmacol Biochem Behav* 59:859-872.
- Hanus L, bu-Lafi S, Fride E, Breuer A, Vogel Z, Shalev DE, Kustanovich I, Mechoulam R (2001) 2-arachidonyl glyceryl ether, an endogenous agonist of the cannabinoid CB1 receptor. *Proc Natl Acad Sci U S A* 98:3662-3665.
- Heffner TG, Hartman JA, Seiden LS (1980) A rapid method for the regional dissection of the rat brain. *Pharmacol Biochem Behav* 13:453-456.
- Herin DV, Liu S, Ullrich T, Rice KC, Cunningham KA (2005) Role of the serotonin 5-HT2A receptor in the hyperlocomotive and hyperthermic effects of (+)-3,4-methylenedioxymethamphetamine. *Psychopharmacology (Berl)* 178:505-513.

- Herkenham M, Lynn AB, De Costa BR, Richfield EK (1991a) Neuronal localization of cannabinoid receptors in the basal ganglia of the rat. *Brain Res* 547:267-274.
- Herkenham M, Lynn AB, Johnson MR, Melvin LS, De Costa BR, Rice KC (1991b) Characterization and localization of cannabinoid receptors in rat brain: a quantitative in vitro autoradiographic study. *J Neurosci* 11:563-583.
- Hohmann AG, Briley EM, Herkenham M (1999) Pre- and postsynaptic distribution of cannabinoid and mu opioid receptors in rat spinal cord. *Brain Res* 822:17-25.
- Huang MH, Bahl JJ, Wu Y, Hu F, Larson DF, Roeske WR, Ewy GA (2005) Neuroendocrine properties of intrinsic cardiac adrenergic cells in fetal rat heart. *Am J Physiol Heart Circ Physiol* 288:H497-H503.
- Hurley MJ, Mash DC, Jenner P (2003) Expression of cannabinoid CB1 receptor mRNA in basal ganglia of normal and parkinsonian human brain. *J Neural Transm* 110:1279-1288.
- Ikemoto S, Kohl RR, McBride WJ (1997a) GABA(A) receptor blockade in the anterior ventral tegmental area increases extracellular levels of dopamine in the nucleus accumbens of rats. *J Neurochem* 69:137-143.
- Ikemoto S, Murphy JM, McBride WJ (1997b) Self-infusion of GABA(A) antagonists directly into the ventral tegmental area and adjacent regions. *Behav Neurosci* 111:369-380.
- Jiang W, Zhang Y, Xiao L, Van CJ, Ji SP, Bai G, Zhang X (2005) Cannabinoids promote embryonic and adult hippocampus neurogenesis and produce anxiolytic- and antidepressant-like effects. *J Clin Invest* 115:3104-3116.
- Johnson SW, North RA (1992a) Opioids excite dopamine neurons by hyperpolarization of local interneurons. *J Neurosci* 12:483-488.
- Johnson SW, North RA (1992b) Two types of neurone in the rat ventral tegmental area and their synaptic inputs. *J Physiol* 450:455-468.
- Julian MD, Martin AB, Cuellar B, Rodriguez De FF, Navarro M, Moratalla R, Garcia-Segura LM (2003) Neuroanatomical relationship between type 1 cannabinoid receptors and dopaminergic systems in the rat basal ganglia. *Neuroscience* 119:309-318.
- Kalant H (2001) Medicinal use of cannabis: history and current status. *Pain Res Manag* 6:80-91.
- Kalivas PW, Nakamura M (1999) Neural systems for behavioral activation and reward. *Curr Opin Neurobiol* 9:223-227.
- Karanian DA, Bahr BA (2006) Cannabinoid drugs and enhancement of endocannabinoid responses: strategies for a wide array of disease states. *Curr Mol Med* 6:677-684.

- Kelly J, Alheid GF, Newberg A, Grossman SP (1977) GABA stimulation and blockade in the hypothalamus and midbrain: effects on feeding and locomotor activity. *Pharmacol Biochem Behav* 7:537-541.
- Kelly PH, Iversen LL (1975) LSD as an agonist at mesolimbic dopamine receptors. *Psychopharmacologia* 45:221-224.
- Kelly S, Chapman V (2001) Selective cannabinoid CB1 receptor activation inhibits spinal nociceptive transmission in vivo. *J Neurophysiol* 86:3061-3064.
- Keppel (1973) *Design and Analysis, a Researcher's Handbook*. New Jersey: Prentis-Hall.
- Kim E, Clark AL, Kiss A, Hahn JW, Wesselschmidt R, Coscia CJ, Belcheva MM (2006) μ - and κ -Opioids Induce the Differentiation of Embryonic Stem Cells to Neural Progenitors. *J Biol Chem* 281:33749-33760.
- Kim RH, Smith PD, Aleyasin H, Hayley S, Mount MP, Pownall S, Wakeham A, You-Ten AJ, Kalia SK, Horne P, Westaway D, Lozano AM, Anisman H, Park DS, Mak TW (2005) Hypersensitivity of DJ-1-deficient mice to 1-methyl-4-phenyl-1,2,3,6-tetrahydropyridine (MPTP) and oxidative stress. *Proc Natl Acad Sci U S A* 102:5215-5220.
- Kirby MT, Hampson RE, Deadwyler SA (2000) Cannabinoid receptor activation in CA1 pyramidal cells in adult rat hippocampus. *Brain Res* 863:120-131.
- Klitenick MA, DeWitte P, Kalivas PW (1992) Regulation of somatodendritic dopamine release in the ventral tegmental area by opioids and GABA: an in vivo microdialysis study. *J Neurosci* 12:2623-2632.
- Klitenick MA, Wirtshafter D (1995) Behavioral and neurochemical effects of opioids in the paramedian midbrain tegmentum including the median raphe nucleus and ventral tegmental area. *J Pharmacol Exp Ther* 273:327-336.
- Koe BK (1976) Molecular geometry of inhibitors of the uptake of catecholamines and serotonin in synaptosomal preparations of rat brain. *J Pharmacol Exp Ther* 199:649-661.
- Koob GF, Nestler EJ (1997) The neurobiology of drug addiction. *J Neuropsychiatry Clin Neurosci* 9:482-497.
- Korotkova TM, Ponomarenko AA, Brown RE, Haas HL (2004) Functional diversity of ventral midbrain dopamine and GABAergic neurons. *Mol Neurobiol* 29:243-259.
- Kunos G, Batkai S, Offertaler L, Mo F, Liu J, Karcher J, Harvey-White J (2002) The quest for a vascular endothelial cannabinoid receptor. *Chem Phys Lipids* 121:45-56.
- Leite-Morris KA, Fukudome EY, Kaplan GB (2002) Opiate-induced motor stimulation is regulated by gamma-aminobutyric acid type B receptors found in the ventral tegmental area in mice. *Neurosci Lett* 317:119-122.

- Livak KJ, Schmittgen TD (2001) Analysis of relative gene expression data using real-time quantitative PCR and the 2(-Delta Delta C(T)) Method. *Methods* 25:402-408.
- Lopez-Redondo F, Lees GM, Pertwee RG (1997) Effects of cannabinoid receptor ligands on electrophysiological properties of myenteric neurones of the guinea-pig ileum. *Br J Pharmacol* 122:330-334.
- Luo MC, Zhang DQ, Ma SW, Huang YY, Shuster SJ, Porreca F, Lai J (2005) An efficient intrathecal delivery of small interfering RNA to the spinal cord and peripheral neurons. *Mol Pain* 1:1-29.
- Majak K, Pitkanen A (2003) Activation of the amygdalo-entorhinal pathway in fear-conditioning in rat. *Eur J Neurosci* 18:1652-1659.
- Mansour A, Fox CA, Burke S, Akil H, Watson SJ (1995) Immunohistochemical localization of the cloned mu opioid receptor in the rat CNS. *J Chem Neuroanat* 8:283-305.
- Marinelli M, Cooper DC, Baker LK, White FJ (2003) Impulse activity of midbrain dopamine neurons modulates drug-seeking behavior. *Psychopharmacology (Berl)* 168:84-98.
- Marinelli M, White FJ (2000) Enhanced vulnerability to cocaine self-administration is associated with elevated impulse activity of midbrain dopamine neurons. *J Neurosci* 20:8876-8885.
- Mathon DS, Kamal A, Smidt MP, Ramakers GM (2003) Modulation of cellular activity and synaptic transmission in the ventral tegmental area. *Eur J Pharmacol* 480:97-115.
- Matsuda LA, Lolait SJ, Brownstein MJ, Young AC, Bonner TI (1990) Structure of a cannabinoid receptor and functional expression of the cloned cDNA. *Nature* 346:561-564.
- Matthews RT, German DC (1984) Electrophysiological evidence for excitation of rat ventral tegmental area dopamine neurons by morphine. *Neuroscience* 11:617-625.
- McInvale AC, Staudinger J, Harlan RE, Garcia MM (2002) Immunolocalization of PICK1 in the ascending auditory pathways of the adult rat. *J Comp Neurol* 450:382-394.
- Mechoulam R, Ben Shabat S, Hanus L, Ligumsky M, Kaminski NE, Schatz AR, Gopher A, Almog S, Martin BR, Compton DR, . (1995) Identification of an endogenous 2-monoglyceride, present in canine gut, that binds to cannabinoid receptors. *Biochem Pharmacol* 50:83-90.
- Mechoulam R, Gaoni Y (1965a) A total synthesis of dl-delta-1-tetrahydrocannabinol, the active constituent of hashish. *J Am Chem Soc* 87:3273-3275.
- Mechoulam R, Gaoni Y (1965b) Hashish. IV. The isolation and structure of cannabinolic cannabidiolic and cannabigerolic acids. *Tetrahedron* 21:1223-1229.

- Mechoulam R, Hanu L (2001) The cannabinoids: an overview. Therapeutic implications in vomiting and nausea after cancer chemotherapy, in appetite promotion, in multiple sclerosis and in neuroprotection. *Pain Res Manag* 6:67-73.
- Melis M, Pistis M, Perra S, Muntoni AL, Pillolla G, Gessa GL (2004) Endocannabinoids mediate presynaptic inhibition of glutamatergic transmission in rat ventral tegmental area dopamine neurons through activation of CB1 receptors. *J Neurosci* 24:53-62.
- Miller JD, Sanghera MK, German DC (1981) Mesencephalic dopaminergic unit activity in the behaviorally conditioned rat. *Life Sci* 29:1255-1263.
- Moldrich G, Wenger T (2000) Localization of the CB1 cannabinoid receptor in the rat brain. An immunohistochemical study. *Peptides* 21:1735-1742.
- Munro S, Thomas KL, bu-Shaar M (1993) Molecular characterization of a peripheral receptor for cannabinoids. *Nature* 365:61-65.
- Nagai T, McGeer PL, McGeer EG (1983) Distribution of GABA-T-intensive neurons in the rat forebrain and midbrain. *J Comp Neurol* 218:220-238.
- Nikulina EM, Hammer RP, Jr., Miczek KA, Kream RM (1999) Social defeat stress increases expression of mu-opioid receptor mRNA in rat ventral tegmental area. *Neuroreport* 10:3015-3019.
- Nocjar C, Roth BL, Pehek EA (2002) Localization of 5-HT(2A) receptors on dopamine cells in subnuclei of the midbrain A10 cell group. *Neuroscience* 111:163-176.
- O'Brien DP, White FJ (1987) Inhibition of non-dopamine cells in the ventral tegmental area by benzodiazepines: relationship to A10 dopamine cell activity. *Eur J Pharmacol* 142:343-354.
- Onaivi ES, Ishiguro H, Gong JP, Patel S, Perchuk A, Meozzi PA, Myers L, Mora Z, Tagliaferro P, Gardner E, Brusco A, Akinshola BE, Liu QR, Hope B, Iwasaki S, Arinami T, Teasentfitz L, Uhl GR (2006) Discovery of the presence and functional expression of cannabinoid CB2 receptors in brain. *Ann N Y Acad Sci* 1074:514-536.
- Overton PG, Clark D (1997) Burst firing in midbrain dopaminergic neurons. *Brain Res Brain Res Rev* 25:312-334.
- Patel S, Hillard CJ (2003) Cannabinoid-induced Fos expression within A10 dopaminergic neurons. *Brain Res* 963:15-25.
- Paxinos G, Watson C (2005) *The Rat Brain In Stereotaxic Coordinates*. Sydney: Elsevier Academic Press.
- Pertwee RG (1997) Pharmacology of cannabinoid CB1 and CB2 receptors. *Pharmacol Ther* 74:129-180.

- Pettit DA, Harrison MP, Olson JM, Spencer RF, Cabral GA (1998) Immunohistochemical localization of the neural cannabinoid receptor in rat brain. *J Neurosci Res* 51:391-402.
- Phillipson OT (1979) The cytoarchitecture of the interfascicular nucleus and ventral tegmental area of Tsai in the rat. *J Comp Neurol* 187:85-98.
- Phillipson OT, Griffith AC (1980) The neurones of origin for the mesohabular dopamine pathway. *Brain Res* 197:213-218.
- Pickel VM, Chan J, Kash TL, Rodriguez JJ, MacKie K (2004) Compartment-specific localization of cannabinoid 1 (CB1) and mu-opioid receptors in rat nucleus accumbens. *Neuroscience* 127:101-112.
- Pierce RC, Kumaresan V (2006) The mesolimbic dopamine system: the final common pathway for the reinforcing effect of drugs of abuse? *Neurosci Biobehav Rev* 30:215-238.
- Pop E (1999) Cannabinoids, endogenous ligands and synthetic analogs. *Curr Opin Chem Biol* 3:418-425.
- Porreca F, Burgess SE, Gardell LR, Vanderah TW, Malan TP, Jr., Ossipov MH, Lappi DA, Lai J (2001) Inhibition of neuropathic pain by selective ablation of brainstem medullary cells expressing the mu-opioid receptor. *J Neurosci* 21:5281-5288.
- Rodriguez JJ, MacKie K, Pickel VM (2001) Ultrastructural localization of the CB1 cannabinoid receptor in mu-opioid receptor patches of the rat Caudate putamen nucleus. *J Neurosci* 21:823-833.
- Romero J, Berrendero F, Perez-Rosado A, Manzanares J, Rojo A, Fernandez-Ruiz JJ, de Yébenes JG, Ramos JA (2000) Unilateral 6-hydroxydopamine lesions of nigrostriatal dopaminergic neurons increased CB1 receptor mRNA levels in the caudate-putamen. *Life Sci* 66:485-494.
- Rozen S, Skaletsky H (2000) Primer3 on the WWW for general users and for biologist programmers. *Methods Mol Biol* 132:365-386.
- Salio C, Fischer J, Franzoni MF, Conrath M (2002) Pre- and postsynaptic localizations of the CB1 cannabinoid receptor in the dorsal horn of the rat spinal cord. *Neuroscience* 110:755-764.
- Sanchez JF, Crooks DR, Lee CT, Schoen CJ, Amable R, Zeng X, Florival-Victor T, Morales N, Truckenmiller ME, Smith DR, Freed WJ (2006) GABAergic lineage differentiation of AF5 neural progenitor cells in vitro. *Cell Tissue Res* 324:1-8.
- Schatz AR, Lee M, Condie RB, Pulaski JT, Kaminski NE (1997) Cannabinoid receptors CB1 and CB2: a characterization of expression and adenylate cyclase modulation within the immune system. *Toxicol Appl Pharmacol* 142:278-287.

- Schlicker E, Kathmann M (2001) Modulation of transmitter release via presynaptic cannabinoid receptors. *Trends Pharmacol Sci* 22:565-572.
- Schweitzer P (2000) Cannabinoids decrease the K(+) M-current in hippocampal CA1 neurons. *J Neurosci* 20:51-58.
- Seeger G, Hartig W, Rossner S, Schliebs R, Bruckner G, Bigl V, Brauer K (1997) Electron microscopic evidence for microglial phagocytic activity and cholinergic cell death after administration of the immunotoxin 192IgG-saporin in rat. *J Neurosci Res* 48:465-476.
- Shire D, Carillon C, Kaghad M, Calandra B, Rinaldi-Carmona M, Le FG, Caput D, Ferrara P (1995) An amino-terminal variant of the central cannabinoid receptor resulting from alternative splicing. *J Biol Chem* 270:3726-3731.
- Silverdale MA, McGuire S, McInnes A, Crossman AR, Brotchie JM (2001) Striatal cannabinoid CB1 receptor mRNA expression is decreased in the reserpine-treated rat model of Parkinson's disease. *Exp Neurol* 169:400-406.
- Singer JD (1998) Using SAS PROC MIXED to Fit Multilevel Models, Hierarchical Models, and Individual Growth Models. *Journal of Educ and Behavior Statistics* 24:323-355.
- Smith PF, Ashton JC, Darlington CL (2006) The endocannabinoid system: A new player in the neurochemical control of vestibular function? *Audiol Neurootol* 11:207-212.
- Spanagel R, Weiss F (1999) The dopamine hypothesis of reward: past and current status. *Trends Neurosci* 22:521-527.
- Steffensen SC, Svingos AL, Pickel VM, Henriksen SJ (1998) Electrophysiological characterization of GABAergic neurons in the ventral tegmental area. *J Neurosci* 18:8003-8015.
- Sugiura T, Kondo S, Sukagawa A, Nakane S, Shinoda A, Itoh K, Yamashita A, Waku K (1995) 2-Arachidonoylglycerol: a possible endogenous cannabinoid receptor ligand in brain. *Biochem Biophys Res Commun* 215:89-97.
- Swanson LW (1982d) The projections of the ventral tegmental area and adjacent regions: a combined fluorescent retrograde tracer and immunofluorescence study in the rat. *Brain Res Bull* 9:321-353.
- Swanson LW (1982a) The projections of the ventral tegmental area and adjacent regions: a combined fluorescent retrograde tracer and immunofluorescence study in the rat. *Brain Res Bull* 9:321-353.
- Swanson LW (1982b) The projections of the ventral tegmental area and adjacent regions: a combined fluorescent retrograde tracer and immunofluorescence study in the rat. *Brain Res Bull* 9:321-353.

- Swanson LW (1982c) The projections of the ventral tegmental area and adjacent regions: a combined fluorescent retrograde tracer and immunofluorescence study in the rat. *Brain Res Bull* 9:321-353.
- Szabo B, Siemes S, Wallmichrath I (2002) Inhibition of GABAergic neurotransmission in the ventral tegmental area by cannabinoids. *Eur J Neurosci* 15:2057-2061.
- Taber MT, Baker GB, Fibiger HC (1996) Glutamate receptor agonists decrease extracellular dopamine in the rat nucleus accumbens in vivo. *Synapse* 24:165-172.
- Tanda G, Goldberg SR (2003) Cannabinoids: reward, dependence, and underlying neurochemical mechanisms--a review of recent preclinical data. *Psychopharmacology (Berl)* 169:115-134.
- Tanda G, Pontieri FE, Di Chiara G (1997) Cannabinoid and heroin activation of mesolimbic dopamine transmission by a common mu1 opioid receptor mechanism. *Science* 276:2048-2050.
- Tokuno H, Chiken S, Kametani K, Moriizumi T (2002) Efferent projections from the striatal patch compartment: anterograde degeneration after selective ablation of neurons expressing mu-opioid receptor in rats. *Neurosci Lett* 332:5-8.
- Tsou K, Brown S, Sanudo-Pena MC, MacKie K, Walker JM (1998) Immunohistochemical distribution of cannabinoid CB1 receptors in the rat central nervous system. *Neuroscience* 83:393-411.
- Vallano ML, Beaman-Hall CM, Bui CJ, Middleton FA (2006) Depolarization and Ca(2+) down regulate CB1 receptors and CB1-mediated signaling in cerebellar granule neurons. *Neuropharmacology* 50:651-660.
- Van Bockstaele EJ, Pickel VM (1995) GABA-containing neurons in the ventral tegmental area project to the nucleus accumbens in rat brain. *Brain Res* 682:215-221.
- Wang CZ, Johnson KM (2005) Differential effects of acute and subchronic administration on phencyclidine-induced neurodegeneration in the perinatal rat. *J Neurosci Res* 81:284-292.
- Wenger T, Moldrich G, Furst S (2003) Neuromorphological background of cannabis addiction. *Brain Res Bull* 61:125-128.
- White FJ (1996) Synaptic regulation of mesocorticolimbic dopamine neurons. *Annu Rev Neurosci* 19:405-436.
- Wikstrom AC, Bakke O, Okret S, Bronnegard M, Gustafsson JA (1987) Intracellular localization of the glucocorticoid receptor: evidence for cytoplasmic and nuclear localization. *Endocrinology* 120:1232-1242.
- Wiley RG (1992) Neural lesioning with ribosome-inactivating proteins: suicide transport and immunolesioning. *Trends Neurosci* 15:285-290.

- Wilson RI, Nicoll RA (2001) Endogenous cannabinoids mediate retrograde signalling at hippocampal synapses. *Nature* 410:588-592.
- Wilson RI, Nicoll RA (2002) Endocannabinoid signaling in the brain. *Science* 296:678-682.
- Wise RA (1998) Drug-activation of brain reward pathways. *Drug Alcohol Depend* 51:13-22.
- Wise RA (2005) Forebrain substrates of reward and motivation. *J Comp Neurol* 493:115-121.
- Wise RA, Bozarth MA (1987) A psychomotor stimulant theory of addiction. *Psychol Rev* 94:469-492.
- Xi ZX, Stein EA (1999) Baclofen inhibits heroin self-administration behavior and mesolimbic dopamine release. *J Pharmacol Exp Ther* 290:1369-1374.
- Yamamoto T, Takada K (2000) Role of cannabinoid receptor in the brain as it relates to drug reward. *Jpn J Pharmacol* 84:229-236.
- Yuan JS, Reed A, Chen F, Stewart CN, Jr. (2006) Statistical analysis of real-time PCR data. *BMC Bioinformatics* 7:85.
- Zangen A, Solinas M, Ikemoto S, Goldberg SR, Wise RA (2006) Two brain sites for cannabinoid reward. *J Neurosci* 26:4901-4907.

VITA

Erik Justin Shank was born in Landstuhl, Germany on April 5, 1975 to Captain John and Angela Shank. He completed a B.S. in Marine Biology at Texas A&M University in 1998 with the equivalency of a minor in chemistry. He then volunteered at the HIV Pathogenesis Research Laboratory to gain critical laboratory skills and rapidly became a lead research technician. He then matriculated into the UTMB Pharmacology Graduate Program in 2001. Additionally, he was awarded a National Institute for Drug Abuse Individual National Research Service Award and was a recipient of a College on Problems of Drug Dependence travel award used to present his findings at national and international meetings. He was also instrumental in the development the Pharmacology and Toxicology student organization and served as the first president, representing the students of the Pharmacology and Toxicology graduate program.

Education

B.S., December 1998, Texas A&M University, Galveston, TX

Publications

Shank, EJ, and Cunningham, KA (2006). Localization of Cannabinoid CB1 Receptors in Subnuclei of the Ventral Tegmental Area. *J. Comp. Neurology*, submitted.

Shank, EJ, Seitz, PK, Stutz, SJ, and Cunningham, KA (2006) Selective ablation of neurons expressing μ -opioid receptors in the ventral tegmental area transiently increases basal locomotor activity and cocaine-evoked activity in rats. *Behavior Neurosci*, Submitted.